# Lithospheric unzipping explaining hot orogenesis during continental subduction

Douwe J.J. van Hinsbergen[1], Thomas N. Lamont[2,3], Carl Guilmette[4]

1. Department of Earth Sciences, Utrecht University, Princetonlaan 8A, 3584 CB Utrecht, Netherlands
2. School of Earth Sciences, Wills Memorial Building, University of Bristol, Bristol, 26 BS81RL, UK
3. Department of Geoscience, University of Nevada, Las Vegas, NV, USA
4. Département de Géologie et de Génie Géologique, Université Laval, Québec, QC, Canada

Corresponding author: D.J.J. van Hinsbergen, d.j.j.vanhinsbergen@uu.nl

*THIS MANUSCRIPT HAS NOT BEEN ACCEPTED FOR PUBLICATION YET.

IT IS RESUBMITTED AFTER PEER REVIEW AND REVISION TO 'TECTONICS'.*

**Key Points**

-The Aegean-Anatolian orogen contains 20-35 km thick continental nappes that underwent syn-burial Barrovian metamorphism

-We explain this by lithospheric unzipping at the Moho: the crust underthrusted the upper plate, the mantle lithosphere subducted

-Lithospheric unzipping may have been the default geological response to continental subduction in the Proterozoic

**ABSTRACT**

Phanerozoic accretionary orogens typically contain upper crustal nappes derived from subducted lithosphere - oceanic or continental - that display (ultra-)high-pressure, low-temperature ((U)HP-LT) metamorphism. Surprisingly, such orogens often also contain coeval continent-derived nappes that underwent ‘Barrovian’ (MP-HT) syn-burial metamorphism instead. Here, we show examples from the eastern Mediterranean orogen of such Barrovian nappes, which were transported at a low angle below the orogenic crust over 150 km or more within ~10 Ma after the inception of their underthrusting. These Barrovian nappes - the Kırşehir Block, Menderes Massif and Naxos Basal Unit - form the deepest exposed structural levels of the orogen and are still underlain by 20-35 km thick continental crust. However, they are missing their pre-orogenic lithospheric mantle, which forms part of steeply subducted slabs instead. We propose that these Barrovian nappes were accreted by a syn-subduction delamination process dubbed 'lithospheric unzipping', whereby continental crust decoupled around Moho depth from its steeply subducting mantle lithosphere, and underplated the accretionary orogen at low angle. The unzipped crust, no longer protected from the asthenosphere by mantle lithosphere, heated up quickly while underthrusting the orogen, pushed by the slab. We propose that continental subduction may thus have three modes: (i) formation of thin (U)HP-LT nappes during subduction of stretched continental margins; (ii) underplating of thicker, MP-HT continental crust by unzipping; and (iii) eventual arrest of continental subduction with the arrival of unstretched continent. Finally, the process of lithospheric unzipping may have been the default geological response to continental subduction in a hotter, younger Earth, possibly explaining enigmatic hot Proterozoic orogenesis, such as in the Trans-Hudson orogen of Canada.

**PLAIN LANGUAGE SUMMARY**

When oceanic plates and the edges of continents, which consist of a layer of crust overlying a layer of mantle lithosphere, enter subduction zones, they are rapidly buried. As a result, such subducted rocks experienced high pressures, but relatively low temperatures, because rocks did not have time to heat up. Surprisingly, however, the deepest rock units of the mountain belt of Greece and Turkey, which contains continental crust that was once part of the subducted ‘Greater Adria’ continent, experienced very high temperatures and only medium pressures during their burial, but why they were became so hot is ill-understood. We show here that these rocks were transported at a low angle, as far as 150-200 km below the overriding plate. We explain these observations by a process of ‘lithospheric unzipping’: when thin continental crust enters subduction zones, it is steeply dragged down into a subduction zone, but when thicker crust arrives, it ‘unzips’: the crust splits from the mantle lithosphere and is shoved at low angle between the upper plate and the underlying hot mantle, causing heating. The mantle lithosphere subducts steeply, and keeps the subduction process and associated arc magmatism going. We show examples from the 2 billion-year-old Trans-Hudson mountain belt of Canada that may show that lithospheric unzipping may have been the default response to continental subduction in the hotter, younger Earth.

## 1. Introduction

The analysis of metamorphic rocks in orogenic belt provides quantitative constraints on the dynamics of subduction and mountain building processes, and changes therein throughout Earth history (Brown and Johnson, 2018). Rocks that become buried in a subduction zone typically undergo (ultra) high-pressure metamorphism ((U)HP) due to rapid deep burial, but at relatively low-temperature (LT) because heating of rocks, by conduction, radioactive heat production and fluid or magma advection, takes time (Brown, 1993; 2007; Jamtveit and Austrheim, 2010). Such HP-LT metamorphism generates cool geotherms (20-40°C/kbar) and is common in accretionary orogens that form by the episodic transfer of rock units within discrete, up to a few km thick thrust sheets (nappes) from a subducting oceanic or continental lithosphere to an overriding plate lithosphere (Cawood et al., 2009; van Hinsbergen and Schouten, 2021). Contrasting high-temperature (HT) metamorphism at moderate pressures (MP) (‘Barrovian’, ~60-100 °C/kbar) typically post-dates and overprints HP-LT metamorphism and occurs when accreted nappes and thickened crust thermally equilibrate following conduction relaxation of isotherms (typically on timescales of tens of millions of years timescales (England and Thompson, 1984; Glazner and Bartley, 1985; Jamieson et al., 1998; Lamont et al., 2023b; Smye et al., 2011), or when they become disturbed by magmatic intrusion or asthenospheric upwelling (Brown, 1993; 2007; Jolivet et al., 2015; Platt and Vissers, 1989). A well-known accretionary region with HP-LT metamorphic belts, often overprinted by younger Barrovian heating, is the eastern Mediterranean orogen in Greece and Turkey (Jolivet et al., 2003; 2015; Okay and Whitney, 2010) (Figure 1). However, the eastern Mediterranean orogen contains three puzzling cases, where nappes deep in the orogenic structure appear to have escaped the HP-LT stage and underwent syn-burial Barrovian metamorphism instead, along-strike from nappes that simultaneously experienced HP-LT metamorphic conditions in the same subduction zone.

The eastern Mediterranean orogen contains accreted rock units derived from subducted African plate lithosphere that was partly oceanic but also for a large part continental in nature (van Hinsbergen et al., 2005a; 2016). Continental subduction produced regionally extensive nappes (Fig. 1) whose age of burial is well-constrained from their youngest sediments and their oldest metamorphic ages (Jolivet and Brun, 2010; van Hinsbergen et al., 2005a; b). Coeval prograde HP-LT or Barrovian metamorphism are recorded within those nappes along-strike in the orogen, on short distances (~100 km), and throughout orogenic history (Figure 1): (i) The eclogite-facies, HP-LT Tavşanlı zone of western Turkey was buried at the same time (90-80 Ma) (Mulcahy et al., 2014; Pourteau et al., 2019) as the Kırşehir Massif of central Turkey that underwent Barrovian syn-burial conditions (van Hinsbergen et al., 2016; Whitney and Hamilton, 2004); (ii) the Eocene Cycladic Blueschist unit of central Greece was buried to HP-LT conditions and accreted between ~55-35 Ma (Ring et al., 2007; Kotowski et al., 2022; see also data compilation in Philippon et al., 2012), overlapping with the burial and accretion of MP-HT Menderes Massif of western Turkey (Lips et al., 2001; Bozkurt et al., 2011; Schmidt et al., 2015); and (iii) the HP-LT Phyllite-Quartzite and Plattenkalk units of Crete and the Peloponnesos (Jolivet et al., 1996; 2010b) were buried coevally (25-15 Ma) with the syn-burial Barrovian Basal Unit of Naxos (Lamont et al., 2020c; 2023b). Previous explanations for the along-strike differences in prograde metamorphic conditions mostly concentrated on one of the three cases and invoked lateral variation in crustal thickening or thinning, mantle delamination, subduction obliquity, subduction and roll-back rates, or dramatic changes in the subduction zone geometry (slab break-off or tearing, transferral, of subduction) (Jolivet et al., 2010b; 2015; Lamont et al., 2020a; Plunder et al., 2018; van Hinsbergen et al., 2010), but none of these explanations apply to all three cases. Alternatively, Ring et al. (2009) and Gessner et al. (2013) pointed out that along-strike variation in paleogeographic distribution of continental crust and its thickness, and its response to burial in a subduction zone may have played a role. In this paper, we explore this avenue, building on a recent detailed reconstruction of pre-orogenic Mediterranean paleogeography (van Hinsbergen et al., 2020).

Here, we review the tectonic setting and history of the nappes that underwent these contrasting metamorphic histories. We use the previous conceptual explanations as guide for our review, which concentrates on pressure-temperature-time constraints of the three contrasting metamorphic pairs, identify their structural position in the modern orogenic architecture, the interpreted history of structurally higher units, and their position relative to the subduction zone(s) that accommodated Africa-Europe convergence through time. We aim to develop a concept that may explain all three cases and we will discuss how the eastern Mediterranean cases may help using orogenic geological records elsewhere and in deep geological time to decipher subduction history and evolution.

## 2. Review

### *2.1 Plate tectonic setting and regional eastern Mediterranean orogenic architecture*

The eastern Mediterranean orogen is an accretionary orogen that consists of overall E-W trending nappes that were were accreted from now-subducted oceanic and continental lithosphere of the African plate. At present, only one subduction zone is accommodating Africa-Eurasia convergence in the eastern Mediterranean region (Figure 1). However, in the Jurassic and Cretaceous, convergence was partitioned over multiple subduction zones, including intra-oceanic ones that existed within the Neotethyan Ocean that then still intervened Africa and Eurasia. Relics of the overriding oceanic plates of those intra-oceanic subduction zones are now found as Jurassic and Cretaceous ophiolites that overlie the accreted and partly metamorphosed nappes (Robertson, 2002).

The timing of accretion, and associated regional, syn-burial metamorphism of the nappes generally gets younger structurally downwards in the orogenic structure, and geographically southwards. The orogen is complex, curved, and its architecture is laterally variable (Figure 1). This lateral variability is on the one hand the result of lateral appearance and disappearance of nappe units that result from the paleogeographic distributions of continental and oceanic lithosphere of the subducted African plate lithosphere (Dercourt et al., 1986; Stampfli and Hochard, 2009; van Hinsbergen et al., 2020). On the other hand, it results from widespread upper plate extension - in the late Cretaceous to Eocene in Central Anatolia, and Eocene and younger in the Aegean region - that led to widespread exhumation of previously buried and metamorphosed portions of the nappes (Gautier et al., 1999; 2008; Jolivet and Brun, 2010; Gürer et al., 2018).

Nappe stacking resulted in significant crustal thickening: in regions unaffected by later extension such as in western Greece, or the Tauride fold-thrust belt, the crust is still up to 40-45 km (Abgarmi et al., 2017; Cossette et al., 2016; Delph et al., 2017; McPhee et al., 2022). However, this thick crust is underlain by only a thin mantle lithosphere, as shown for instance in the Central Aegean and eastern Anatolian regions (Abgarmi et al., 2017; Barazangi et al., 2006;

Endrun et al., 2011; McPhee et al., 2022). This is likely because the original, pre-orogenic lithospheric underpinnings that existed below the nappes has subducted (Handy et al., 2010; Jolivet and Brun, 2010; van Hinsbergen et al., 2005a; 2010; 2024): these subducted lithospheric underpinnings now forms slabs that are well-imaged with seismic tomography as coherent bodies of lithosphere that penetrate as deep as the mid-mantle (Berk Biryol et al., 2011; Hafkenscheid et al., 2006; van Hinsbergen et al., 2005a).

Because subduction was dominantly north-directed, the northern parts of nappes accreted below the orogen and were hence buried and metamorphosed, whereas the southern parts often escaped metamorphism and accreted at the front of the orogen. The metamorphosed portions of the nappes, discussed in this paper, are exposed in the extensional windows in the center of the orogen (Bonneau, 1984; Lister et al., 1984; Hetzel et al., 1995; Gürer et al., 2018; van Hinsbergen et al., 2005a; Jolivet and Brun, 2010; Ozgul, 1976) (Figure 1).

### *2.2 Nappes with synchronous but contrasting syn-burial metamorphic histories*

#### 2.2.1 Tavşanlı Zone versus the Kırşehir Block

The Tavşanlı Zone of NW Turkey is a 300 km long and 50 km wide belt of folded and thrusted, blueschist to eclogite-facies, Paleo- and Mesozoic metapelitic schists, metavolcanics, and marbles derived from the now-subducted stretched Greater Adriatic continental margin (Okay, 2002) (Figure 1). Above these metamorphosed rocks is formed by regionally extensive ophiolites that are found as highest structural unit across the central and southern Anatolian orogen. These ophiolites that are thought to represent remnants of an oceanic plate below which the Greater Adriatic continental margin was underthrusted (e.g., Plunder et al., 2016; Pourteau et al., 2016; van Hinsbergen et al., 2020). These ophiolites have 'supra-subduction zone' (SSZ) geochemical signatures that suggests that the formed by spreading above a subduction zone (e.g., Robertson, 2002). Welded to the base of these ophiolites, metamorphic soles are found that are thought to have formed at the subduction interface in early stages of subduction (e.g., Dilek & Whitney, 1997; Plunder et al., 2016). Across Turkey $^{40}Ar/^{39}Ar$ cooling ages of metamorphic sole rocks coincide with the magmatic crustal ages of overlying ophiolites, which systematically cluster between ~93 and 90 Ma (Robertson, 2002; Parlak, 2016; van Hinsbergen et al., 2016) - a trend that is systematic in SSZ ophiolites worldwide (van Hinsbergen et al., 2015). Lu/Hf garnet geochronology from a metamorphic sole in an ophiolite above the eastern Tavşanlı massif, however, yielded a 104 Ma age (Pourteau et al., 2019), showing that the subduction zone above which the ophiolites formed, and that eventually buried the Tavşanlı massif, formed ~10 million years before upper plate spreading formed the Anatolian SSZ ophiolites (a correlation also found elsewhere, e.g., in Oman and southern Tibet, Guilmette et al., (2018; 2023)). The magmatic crust of the ophiolite klippen immediately above the Tavşanlı zone has not been dated, but metamorphic sole rocks below these ophiolites yielded hornblende $^{40}Ar/^{39}Ar$ ages of 93-90 Ma (Önen, 2003; Önen and Hall, 1993).

The Tavşanlı Zone became buried to pressures up to 24 kbar at temperatures up to ~500°C (~20°C/kbar) (Davis and Whitney, 2008; Okay, 2002; Plunder et al., 2013) (Figure 2). Lu/Hf geochronology on garnet and lawsonite gave ages interpreted as the timing of burial metamorphism of 91-83 Ma (Mulcahy et al., 2014; Pourteau et al., 2019), showing that subduction of the Tavşanlı Zone occurred soon after, or even partly during supra-subduction zone (SSZ) ophiolite spreading in the upper plate. The Tavşanlı Zone is a few km thick and overlies a younger passive margin-derived nappe, the Afyon Zone, metamorphosed at ~10 kbar/350-400°C (~35-40°C/kbar) around 70-65 Ma (Pourteau et al., 2013), following ~15 Ma of subduction of which no accreted relics are known (van Hinsbergen et al., 2016). The Tavşanlı Zone became intruded by arc plutons of 60-50 Ma, in places associated with a local Barrovian (MP-HT) metamorphic overprint (Seaton et al., 2014). These arc plutons formed after the Afyon Zone accreted and the trench consequently had stepped southwards, bringing the Tavşanlı Zone into the arc position, ~30-40 Ma after its initial underthrusting and accretion.

To the east and southeast of the Tavşanlı Block, the Kırşehir Block of central Turkey exposes greenschist to granulite-facies, Paleo-Mesozoic metapelites, metavolcanics, and marbles overlying a Precambrian crystalline basement (Whitney and Hamilton, 2004). The Kırşehir Block is overlain by widespread, but small ophiolitic klippen with supra-subduction zone geochemistry that yielded U/Pb zircon plagiogranite ages of 90.5 ± 0.2 Ma and 89.4 ± 0.6 Ma (in the Sarıkaraman Ophiolite that overlies the Kırşehir Massif (van Hinsbergen et al., 2016)), collectively known as the Central Anatolian ophiolites (Yalınız et al., 1996; Floyd et al., 2000;

Yaliniz, 2008). Similar to the ophiolites overlying Tavşanlı, these are interpreted as relics of an originally oceanic upper plate that formed above the same subduction zone that buried the Kırşehir Block. Paleomagnetic analysis showed that sheeted dykes in the Sarıkaraman Ophiolite were originally N-S trending suggesting E-W spreading - a pattern that is consistent throughout the eastern Mediterranean Cretaceous ophiolites (Maffione et al., 2017; van Hinsbergen et al., 2016). This is explained by roll-back of N-S trending segments that linked up by E-W trending segments of an intra-oceanic subduction zone that reactivates fracture zones and structures parallel to the passive margin of Greater Adria (van Hinsbergen et al., 2016; 2020). The Kırşehir Block underthrusted obliquely at such a N-S segment, whereas the Tavsanli Zone underthrusted at an E-W striking segment (van Hinsbergen et al., 2016). After underthrusting and accretion, the upper plate oceanic lithosphere was extensionally dismembered and eroded until only the modern Central Anatolian Ophiolite klippen remain (e.g., Gautier et al., 2008; Lefebvre et al., 2011; 2015; van Hinsbergen et al., 2016).

The Kırşehir Block now consists of three submassifs that rotated relative to each other accommodated by Cenozoic fault zones that experienced shortening and strike-slip faulting, forming a NW-ward convex orocline (Advokaat et al., 2014; Lefebvre et al., 2013). Restoring this orocline shows that the Kırşehir Block formed a ~150 km wide (E-W) to ~500 km long (N-S), elongated continental fragment. During regional amphibolite-facies metamorphism, a pervasive, flat-lying foliation formed that systematically recorded top-to-the-SSW sense of shear (Lefebvre, 2011; Lefebvre et al., 2013). Metamorphic conditions in the Kırşehir Block reached peak pressures of 7-8 kbar at temperatures of ~700 °C (~95°C/kbar) in the central of the three sub-massifs, and 5-6 kbar at 700°C (125°C/kbar) in the southern (Lefebvre et al., 2015; Whitney and Dilek, 1998; Whitney and Hamilton, 2004; Whitney et al., 2003) (Figure 2). There is no evidence for a preceding HP-LT metamorphic phase. The oldest ages from the metamorphic rocks of the Kırşehir Block include 91±2 Ma U/Pb zircon ages from migmatites of the Niğde Massif in the south, and a 84.1± 0.8 Ma monazite age from a gneiss in the central Kirsehir Massif that is interpreted as post-peak-metamorphic cooling (Whitney and Hamilton, 2004; Whitney et al., 2003). These ages are partly overlapping with the crystallization ages of the regionally overlying SSZ ophiolites (90.6±0.1 Ma and 89.2±0.4 Ma U/Pb zircon ages) that lie on the Kırşehir Massif (van Hinsbergen et al., 2016).

The restored regional, syn-Barrovian top-to-the-SSW sense of shear recorded throughout the Kırşehir Block metamophics is parallel to the Africa-Europe convergence direction in this time interval and is thus consistent with deformation during underthrusting below the (oceanic) overriding plate (van Hinsbergen et al., 2016). The regional foliation of the Kırşehir Block is cut by a belt of undeformed granitic and gabbroic plutons which have U-Pb zircon ages ranging from 85-70 Ma and geochemical signatures that show that they resulted from both mantle derived arc magmatism and crustal melting (Ilbeyli, 2005; Köksal et al., 2004; van Hinsbergen et al., 2016). The intrusion of the arc plutons and absence of their deformation show that accretion of the Kırşehir Block from the downgoing to the upper plate must have occurred before 85 Ma. The intrusion led to local contact metamorphism (3-4 kbar, ~800°C; Lefebvre et al., 2015) superimposed on regional metamorphism and associated pervasive deformation fabrics. This arc is interpreted to have formed during oceanic subduction that initiated immediately after the Kırşehir Block stopped its underthrusting and accreted to the overriding, oceanic plate lithosphere (Ilbeyli, 2005; Köksal et al., 2004). This means that by ~85 Ma, the Kirsehir Block was located in an upper plate position that was sufficiently far from a trench so that it became intruded by an arc. Typical arc-trench distances are ~150-200 km, Stern (2002), and in the case of central Anatolia, the kinematically restored distance at 85-70 Ma is ~175 km (van Hinsbergen et al., 2020).

After accretion, the Kırşehir Block exhumed along extensional detachments between 85 and 70 Ma. Similar to the extension direction forming the Central Anatolian Ophiolites, these detachments also accommodated E-W extension (Advokaat et al., 2014; Isik et al., 2008; Isik, 2009; Lefebvre et al., 2011; 2015), perpendicular to the reconstructed trench orientation at which the Kırşehir Block underthrusted (van Hinsbergen et al., 2016).

Despite this extension, the crust of the Kırşehir Block has a present-day thickness of ~35 km (Tezel et al., 2013). The block underwent some thickening due to Oligocene shortening (Advokaat et al., 2014; Gülyüz et al., 2013; Lefebvre et al., 2013), and also arc magmatism may likely thickened the crust (Göğüş et al., 2017), but upper Cretaceous sediments that overlie the Kırşehir Block are terrestrial, showing that its crust after accretion was likely tens of km thick even during regional extensional exhumation (Advokaat et al., 2014). There are no tectonic windows in the Kırşehir Block that show that the younger nappes of the Afyon Zone and the

Taurides that fringe the Kırşehir Block to the south (McPhee et al., 2018; Okay et al., 1996) (Figure 1) regionally underlie the block. It is thus likely that the Kırşehir Block was accreted with most if not all of its pre-orogenic crust intact. After 85 Ma, subduction and arc magmatism continued, without accretion, until underthrusting of the Afyon zone around 70-65 Ma (Pourteau et al., 2013; van Hinsbergen et al., 2016). The Afyon zone accreted against the Kırşehir Block and Tavşanlı zone to the south, i.e. some 15 Ma after their climax metamorphism, and the Afyon zone was everywhere metamorphosed under similar HP-LT conditions (~35-40 °C/kbar) with no significant along-strike variation (Candan et al., 2005; Pourteau et al., 2010; 2013). After accretion of the Afyon Zone, and during the formation of the Tauride fold-thrust belt to the south, upper plate extension continued and widespread sedimentary basins formed in which terrestrial to shallow marine sedimentation occurred in Paleocene-Eocene time (Gürer et al., 2016; 2018; Seyitoğlu et al., 2017).

The geological architecture and history above thus suggests an atypical sequence of events. Given the short time spans between the onset of subduction (at or slowly before 104 Ma, Pourteau et al., 2019), supra-subduction zone ophiolite spreading (active until at least ~89 Ma, van Hinsbergen et al., 2016) and Kirsehir Block underthrusting (starting before ~91 Ma and ending before ~84 Ma (Whitney and Hamilton, 2004; Whitney et al., 2003), and the onset of arc magmatism in the Kırşehir Block (~85 Ma (Ilbeyli, 2005; Köksal et al., 2004; van Hinsbergen et al., 2016), these phenomena are best be explained by a tectonic history of one subduction zone only - there is simply insufficient plate convergence, or evidence, to infer yet another one (van Hinsbergen et al., 2016). This would then require that (i) the Kırşehir Block was buried in a subduction zone below oceanic lithosphere shortly after the initiation of that subduction zone; (ii) during the beginning of underthrusting, the upper plate was still undergoing extension, hosting a supra-subduction zone spreading center; (iii) The Kırşehir Block underthrusted for some 6 Ma or slightly longer while undergoing regional Barrovian metamorphism and escaping high-pressure metamorphism, requiring low-angle underthrusting, and (iv) after underthrusting and accretion, the Kırşehir Block was located 175 km from the trench that consumed oceanic lithosphere that intervened the Kırşehir Block from continental units farther south and west (van Hinsbergen et al., 2016). This requires that the Kırşehir Block underthrusted almost horizontally over some 175 km below the upper oceanic lithosphere; (v) even though some crustal thickening may have resulted from intrusion of the 85-70 Ma arc, it is likely that much of the original pre-subduction crust of the Kırşehir Block accreted; and (vi) when the Kırşehir Block stopped underthrusting and accreted below the ophiolites, the slab that fed the arc must already have been present at the typical 100-150 km depth interval to provide fluids for arc melting below the block (van Hinsbergen et al., 2016). This suggests that the mantle lithosphere of the Kırşehir Block subducted steeply into the asthenosphere while the crust did not.

### 2.2.2 Cycladic Blueschist versus Menderes Massif

The Cycladic Blueschist (CBS) comprises a series of nappes that collectively represent a few km structural thickness, which is exposed on the Cycladic Islands and on the Aegean mainland (Jolivet and Brun, 2010; Glodny and Ring, 2022). The upper parts of the CBS are oceanic crust-derived and comprise metabasalts enclosed in serpentinite, which overthrust nappes consisting of a Palaeozoic crystalline basement overlain by Triassic mafic volcanics, and a metasedimentary sequence of presumably deep-marine origin (Bröcker and Pidgeon, 2007; Kotowski and Behr, 2019). The deepest parts of the CBS comprise continental shelf facies metasedimentary rocks, correlated with the pelagic carbonates and cherts that formed in the Pindos Zone of the external Hellenides from the late Triassic onwards that was since then underlain by strongly thinned continental lithosphere (Bonneau, 1984; Schmid et al., 2020). On the island of Naxos, and also elsewhere in the Cyclades, some of the blueschist units contain metabauxites (interpreted to be paleosol erosional surfaces) showing that also shallow-marine rocks were buried deeply (Feenstra, 1985). It is important to note, however, that HP-LT metamorphism of the CBS is only identified in the higher structural units of Naxos (the Zas unit of Lamont et al., 2020c). Deeper structural units however, contain no evidence for HP-LT metamorphism but only display Barrovian, amphibolite-facies metamorphism. These include the intermediate, or Koronos unit that consists of shallow-marine marbles with frequent meta-bauxites, and the lower, or Core Unit that consists of Paleozoic basement granites that underwent Miocene migmatization at kyanite to sillimanite grade conditions (Lamont et al., 2020c, and references therein). We correlate these to the Basal Unit, which includes a continental plate stratigraphy with Paleozoic crystalline basement, passive margin meta-clastics and volcanics, a marble platform sequence, and an

Oligocene meta-foreland basin sequence (Ring et al., 2001; Schmid et al., 2020, and references therein). The Basal Unit thus underthrusted the CBS in Oligocene to Early Miocene time (Lamont et al., 2020c; 2023b; Ring et al., 2007a; Schmid et al., 2020).

The CBS nappes experienced blueschist to eclogite-facies metamorphism (up to 18-23 kbar, 500-600°C, ~20-30 °C/kbar) (Behr et al., 2018; Lamont et al., 2020b; Laurent et al., 2017; Skelton et al., 2019; Wolfe et al., 2023) (Figure 2) and returned U/Pb and Lu/Hf ages between ~55-35 Ma, of which the rocks with continental protoliths recorded ages from ~48 Ma onwards (Dragovic et al., 2012; Gorce et al., 2021; Kotowski et al., 2022; Lagos et al., 2007; Lamont et al., 2023b; Peillod et al., 2017; Tomaschek, 2003; Tual et al., 2022; Uunk et al., 2022), younging structurally downwards (Kotowski et al., 2022). The first phase of regional exhumation of the CBS, during which it was in places retrogressed under greenschist-facies conditions, occurred between ~40 and 20 Ma while the CBS was being underthrusted by the Basal Unit (Cisneros et al., 2021; Jolivet and Brun, 2010; Lamont et al., 2020c; 2023b; Ring et al., 2007a; Searle and Lamont, 2020; Glodny and Ring, 2022). During much of the underthrusting of the CBS, there was no arc magmatism, which only commenced around ~35 Ma in northern Greece and southern Bulgaria after a lull since the late Cretaceous (Pe-Piper and Piper, 2002; Zimmerman et al., 2008). Upon ongoing nappe accretion and upper plate extension, the arc migrated southwards and arrived in the CBS region around 7 Ma (Ersoy and Palmer, 2013). Around ~15-12 Ma, plutons had already intruded both the CBS and Basal Unit, but these related to crustal melting, and caused local contact metamorphism (Jolivet and Brun, 2010; Jolivet et al., 2003; Lamont et al., 2023a).

To the east of the Cyclades, a series of Eocene metamorphosed nappes is exposed in western Turkey, which were underthrusted below the Afyon Zone (Fig 1). These are exposed in the Menderes Massif, a major extensional window that separated the deeper-buried, HP-LT metamorphic Afyon and Tavşanlı zones to the north from their shallower-buried, lower-pressure to non-metamorphic equivalents exposed in SW Turkey, known as the Lycian Nappes (Collins and Robertson, 2003) (Figure 1). To the west, the Afyon Unit disappears, and the highest nappe of the western part of the Menderes Massif is the Selçuk Nappe that consists of a ophiolite melange, which overlies the Dilek Nappe that contains a passive continental margin sequence and that underwent comparable, HP-LT metamorphic conditions as the CBS (500°C/15 kbar;

~30°C/kbar) (Rimmelé et al., 2003; Ring et al., 2007b), but only represents the older part of the CBS metamorphic age spectrum, from 57-44 Ma (Pourteau et al., 2013; Çetinkaplan et al., 2020). The deeper part of the nappe stack in western Turkey consists of the Menderes Nappes, which contain Precambrian crystalline basement and a Paleozoic to Eocene meta-clastic and meta-carbonate sedimentary series with platform carbonate fossils (nummulites, rudists) (Bozkurt and Oberhänsli, 2001; Gessner et al., 2001; Özer and Sözbilir, 2003). Between ~46 and 35 Ma, the Pindos and Menderes nappes thus underthrusted and metamorphosed simultaneously, side by side in the same subduction zone. Their strong lithological differences are paleogeographic in origin: the shallow-water Menderes platform with thick continental crust was separated from deep-water Pindos basin to the west, with probably strongly thinned continental crust by a slope that likely represented a transform fault margin that formed during Triassic Neotethys rifting (van Hinsbergen et al., 2020).

The Menderes Nappes escaped HP-LT metamorphism and instead experienced Barrovian prograde metamorphism. The structurally highest unit is the metasedimentary Selimiye Nappe that underwent the highest grade metamorphism at ~600-650 at 8-11 kbar (Régnier et al., 2003), overlying Precambrian crystalline basement units with Eocene peak metamorphism estimated at up to ~500-550°C at 6-8 kbar (Okay, 2001; Whitney and Bozkurt, 2002) and 625-670°C at 7-9 kbar (Cenki-Tok et al., 2016), i.e. (55-95 °C/kbar) (Figure 2). However, the deepest exposed unit, overthrust by the Precambrian basement, consists of Eocene platform carbonates and underwent only greenschist facies metamorphism (Lips et al., 2001; Gessner et al., 2001). Lu/Hf garnet growth ages show prograde mineral growth between ~42 and 35 Ma (Schmidt et al., 2015), consistent with Rb-Sr ages starting around 45 Ma in the highest-grade, top-most nappes (Bozkurt et al., 2011) and $^{40}Ar$-$^{39}Ar$ syn-metamorphic ages of the basal greenschists of 35 Ma (Lips et al., 2001), i.e. overlapping with the younger part of the CBS HP-LT age spectrum spanning ~55-35 Ma. Within a few Ma after accretion of the Menderes Nappes, late Oligocene arc volcanism occurred immediately to the north of the Menderes Massif (Ersoy and Palmer, 2013), showing that the massif underthrusted the entire west Anatolian forearc. The massif is intruded by granitoids that bear similarities to arc magmas (Akay, 2009; Ozgenc and Ilbeyli, 2008), with ages of ~23-20 Ma and younger (Isik et al., 2004; Ring and Collins, 2005).

The Menderes Massif is still underlain by ~25-30 km thick continental crust (Tezel et al., 2013; Karabulut et al., 2013) and is likely contiguous with the Bey Dağları platform in the non-metamorphic foreland, to the south of the Lycian Nappes (Figure 1). After ~35 Ma, convergence became accommodated at the Hellenic-Cyprus trench to the south of the Bey Dağları platform, consuming oceanic lithosphere of the Eastern Mediterranean Ocean basin, with no exposed accretionary record (van Hinsbergen et al., 2010). Seismic tomographic images of the mantle below western Anatolia reveal a single slab, which detached likely in late Miocene or younger time (Jolivet et al., 2015; van Hinsbergen et al., 2010), that accounts for subduction since the Cretaceous. To explain the present crustal thickness of western Turkey, most of the west-Anatolian crust likely consists of the pre-orogenic continental crustal underpinnings of the deepest Menderes units that decoupled from their subducted mantle lithospheric underpinnings (van Hinsbergen et al., 2010).

#### 2.2.3 Phillite Quartzite/Plattenkalk Units versus Naxos Basal Unit

The Phyllite Quartzite unit (PQ) and the underlying Plattenkalk unit are exposed on Crete and the Peloponnesus in Greece (Figure 1). These are the youngest HP-LT metamorphic nappes of the eastern Mediterranean orogen (Jolivet et al., 1996; Theye et al., 1992). The structurally higher PQ nappe is a few km thick and comprises thin slivers of Paleozoic, pre-Alpine crystalline basement (Romano et al., 2004) overlain by a Carboniferous to Triassic meta-clastic sedimentary series (Krahl et al., 1983) interpreted to reflect a continental passive margin sequence. The unit is interpreted to have been the stratigraphic base of the Tripolitza platform carbonates that are structurally above the PQ units, and which stratigraphically span the Triassic to Oligocene (van Hinsbergen et al., 2005b). The Tripolitza Nappe underlies the Pindos Nappe (i.e., the non-metamorphic equivalent of the Cycladic Blueschist unit). The current contact between the HP-LT PQ Unit and the anchi-metamorphic Tripolitza limestones is an extensional detachment that played a role in the exhumation of the PQ Unit (Jolivet et al., 1996; Rahl et al., 2005). The PQ was buried to up to 18 kbar at ~400°C around 24-20 Ma (~20°C/kbar) (Jolivet et al., 1996; 2010b) (Figure 2). The PQ was thrust upon the Plattenkalk Unit that consists of a Triassic to Oligocene stratigraphy of deep-marine meta-clastic and meta-carbonate sediments and foreland basin clastics that reached metamorphic conditions of 7 kbar and 380°C on Crete (Seidel, 1978) and 7-8.5 kbar at 310-360°C (20-50°C/kbar) on the Peloponnesos (Blumor et al., 1994). The Plattenkalk Unit is correlated to the Ionian zone of the non-metamorphic Aegean foreland (Blumor et al., 1994; Schmid et al., 2020). Because the Plattenkalk Unit reached lower peak-pressure conditions than the overlying PQ unit, part of the exhumation of the PQ must have occurred during the underthrusting of the Plattenkalk. This is interpreted to have occurred in a subduction channel setting along the plate contact, accommodated along detachments at the top of the PQ (Fassoulas et al., 1994; Jolivet et al., 2003; 1996; Thomson et al., 1998; 1999). Since ~15 Ma, exhumation was further aided by multidirectional forearc thinning during regional oroclinal bending (van Hinsbergen and Schmid, 2012; Pastor-Galán et al., 2017), to reach near-surface conditions around 13 Ma, in the late Middle Miocene (Thomson et al., 1998; 1999; Marsellos et al., 2010) and first exposure around 10 Ma (Zachariasse et al., 2011).

Field geological and seismic observations in the foreland of western Greece and the Peloponnesos showed that the underthrusting of the Tripolitza Nappe below the Pindos Nappe, and of the Plattenkalk/Ionian nappes below the Tripolitza Nappe started simultaneously, around 35 Ma (IGRS-IFP, 1966; Sotiropoulos et al., 2003; van Hinsbergen and Schmid, 2012). Simultaneous underthrusting of the Tripolitza/PQ continued throughout the Oligocene and ended in the earliest Miocene, after which Ionian zone underthrusting continued until the late Miocene as shown by the youngest foreland basin deposits on these nappes in western Greece (IGRS-IFP, 1966). Subsequently, the subduction plate contact stepped structurally downward towards the modern Hellenic Trench south of Crete where the thick 'Mediterranean Ridge' accretionary prism formed during subduction of Mesozoic oceanic lithosphere (Kastens, 1991), and structurally deeper into the Adriatic continental foreland in western Greece where the continental Pre-Apulian nappe accreted (Underhill, 1989; van Hinsbergen et al., 2006). The Phyllite-Quartzite unit and Plattenkalk units are still only found in the Aegean forearc, >100 km to the south of the active volcanic arc (Figure 1).

To the north, on mainland Greece (e.g., Fleury and Godfriaux, 1974), and on the Cycladic islands of e.g. Evia (Ring et al., 2007a; Ducharme et al., 2022), Samos (Gessner et al., 2011; Roche et al., 2019), and Naxos (Lamont et al., 2020c; 2023b), the deepest structural is known as the Basal Unit (see Schmid et al., 2020 for a review). Particularly in the central Cyclades where metamorphic overprints are strong, the distinction between the Basal Unit and the overlying Cycladic Blueschist Unit is not everywhere straightforward (see below). However, where metamorphism of the Basal Unit is not high-grade, such as on Samos, shallow marine meta-platform carbonates with bauxite horizons are found with stratigraphic ages that extend into the Eocene, overlain by Oligocene foreland basin clastics (Ring and Layer, 2003). The Basal Unit is therefore correlated to the unmetamorphosed Tripolitza platform carbonates in the Aegean foreland (Fleury and Godfriaux, 1974; see review in Schmid et al., 2020). The distance of the Basal unit exposures to the Tripolitza unit that remained in a foreland position in western Greece, however, is 140 km in western Greece, and up to 400 km in the Cyclades. Even when post-early Miocene extension of the Aegean region is considered, the Basal Unit must have undergone >200 km of underthrusting below the upper plate to reach its modern position (van Hinsbergen and Schmid, 2012). Despite this, pressures reached by the Basal Unit do not exceed ~8-10 kbar, showing that underthrusting must have occurred at very low angles. Temperatures vary strongly across the Basal Unit. On Evia and in Samos, on the northwest and east side of the Cyclades, temperatures of ~350-400°C (35-50°C/kbar) where reached sometime around 20 Ma or shortly thereafter (Ring and Layer, 2003; Ring et al., 2001; Shaked et al., 2000), but on Naxos became much higher.

On Naxos, rocks ascribed to the Basal Unit experienced considerably higher temperatures. The intermediate and deep structural levels of the island that expose shallow-water facies with metabauxite and underlying crystalline basement (Koronos and Core Units of Lamont et al. 2020c) do not show petrological evidence that demonstrate they reached high-pressure conditions, even though they have often been interpreted to be part of the CBS (Martin et al., 2006). The arguments to that end rely on the assumption that the metamorphic rocks on Naxos were all derived from a single nappe, and that ca. 40 Ma rim ages of zircons were derived from the sheared top of the intermediate Koronos unit (Martin et al. 2006; Bolhar et al. 2017). These authors explained the absence of HP-LT metamorphism as the result of an complete overprinting by Miocene Barrovian metamorphism during extension. However, first it is unclear what the 40 Ma date represents as it is not associated with high-pressure metamorphic assemblages, and it post-dates high-pressure conditions in the overlying CBU that were dated at ca. 50 Ma by $^{40}$Ar/$^{39}$Ar geochronology on white mica and hornblende and U-Th-Pb allanite geochronology

(Wijbrans and McDougall, 1987; Lamont et al. 2023b). Second, the dated samples are located on the west side of Naxos close to the Naxos-Paros Detachment, raising the possibility they have been tectonically displaced from the overlying CBU nappe during Miocene extensional shearing and exhumation. Third, and most importantly, Lamont et al. (2020c) demonstrated that garnets in kyanite-bearing assemblages from the Koronos and Core Units recorded prograde garnet growth zoning associated with increasing pressure and temperature from core to rim. This indicates that regional metamorphism that affected these rocks occurred during burial and heating and hence before exhumation. We therefore correlate the Koronos and Core units with a nappe below the CBU, i.e. the Basal Unit. This suggests that the underthrusting of the Basal Unit of Naxos predated the onset of underthrusting of the Tripolitza Unit still exposed in the Hellenic foreland, and paleogeographically to the west, by a few million years, because of lateral paleogeographic contrasts. The Koronos and Core Unit on Naxos underwent prograde metamorphism along an elevated geotherm reaching Barrovian conditions of ~10-11 kbar and ~600-730°C (i.e., 55-73°C/kbar) (Figure 2) dated by U-Pb zircon ages at 20-16 Ma (Keay et al., 2001; Bolhar et al., 2017; Vanderhaege et al., 2018; Lamont et al., 2020c; 2023b). This was followed by partial melting, isothermal decompression and a lower pressure sillimanite grade overprint (5-6 kbar and 670-730°C) at ~16-14 Ma (Lamont et al., 2020c; Ring et al., 2007a; Schmid et al., 2020) and intrusion of crustal derived I and S-type granites at ~15-12 Ma (Altherr, 1988; Jolivet and Brun, 2010; Jolivet et al., 2003; Lamont et al., 2023a). In other words, burial and metamorphism of the Basal Unit occurred sumultaneously with that of the PQ and Plattenkalk units to the south.

Thermochronology also suggest that the Basal Unit was being buried while the overlying Cycladic Blueschist was exhuming along an extensional detachment at the top (Jolivet et al., 2003; Lamont et al., 2020c; 2023b; Ring et al., 2007a; b; Searle and Lamont, 2020). Moreover, exhumation along extensional detachments and associated supra-detachment extensional basins had already been occurring farther north in the Rhodope region since the Eocene and was continuing throughout the Miocene (Brun and Sokoutis, 2007; 2010), showing that the low-angle underthrusting of the Basal Unit below the forearc occurred while the overriding plate was undergoing extension. Around 20 Ma or shortly thereafter, when underthrusting of the Basal Units stopped, it also became exhumed by low-angle normal faults as evidenced by the extreme telescoping of metamorphic stratigraphy and isograds in Western Naxos immediately beneath the Naxos-Paros Detachment (Lamont et al., 2020c).

The continental crust that melted to form the I- and S-type granites of the Cyclades (Altherr et al., 1982; 1988; Pe-Piper, 2000; Lamont et al., 2023a), is likely the 25-26 km thick crust that still underlies the Cyclades (Tirel et al., 2004). Schmid et al. (2020) inferred that crust must somehow have accreted from the subducted African Plate and suggested that it all consists of Ionian (Plattenkalk) crust, which structurally underlies the Tripolitza/PQ units in the external Hellenides and Crete. The Ionian Zone should then have underthrusted most of the Aegean region in tandem with the Tripolitza/Basal Unit. Alternatively, Lamont et al. (2020c; 2023b) and Searle and Lamont (2020) suggested that the Basal Unit is still underlain by its own pre-orogenic crust, and they interpreted that this marks a phase of subduction transferral, with a subducting slab breaking off the Basal Unit lithosphere and a new subduction zone starting to the south. In any case, the crustal thickness of Greece requires that the deepest nappe of the orogen still contains (most of) its original, pre-orogenic crust.

## 3. Discussion

### *3.1 Lithospheric unzipping*

The three case studies above from the Cretaceous to Cenozoic eastern Mediterranean accretionary orogen show that at the same time, and at the same subduction zone, regionally extensive rock units may underthrust at contrasting angles and thus experience contrasting prograde metamorphic evolutions. We identify some key differences between the HP-LT metamorphic units that were buried to depths of up to ~20 kbar under net metamorphic gradients of ~20-40 °C/kbar and stayed close to the subduction zone they were buried in, and the Barrovian units that were buried to pressures of no more than ~8-11 kbar under metamorphic gradients of ~60-100°C/kbar, underthrusting the forearc up to some 200 km from the subduction zone.

The HP-LT units (Tavşanlı, Afyon, Cycladic Blueschist, Phyllite-Quartzite/Plattenkalk Units) are thin nappes, no more than a few km thick, consisting mostly of deep-marine sedimentary cover units of passive continental margin lithosphere, only occasionally still including small fragments of the originally underlying crystalline basement. These HP-LT nappes underwent rapid burial, shown by time gaps between the youngest stratigraphic ages and the oldest metamorphic ages of only some ~10 Ma, and rapid subsequent exhumation, whereby during their exhumation, they thrusted over simultaneously underthrusting younger nappes (Ring et al., 2007a; Searle and Lamont, 2020). The HP-LT nappes may be intruded by arc-derived, or crustal melting-derived plutons, but only after a new forearc crust was built by younger accretion between the HP unit and the trench, tens of Ma after HP metamorphism. Such histories of rapid burial and exhumation close to subduction zones have long been recognized and are commonly explained by buoyancy-driven rise in a subduction channel (Brun and Faccenna, 2008; Jolivet et al., 2003; Platt, 1986; Thomson et al., 1999).

The Barrovian units (Kırşehir Block, Menderes Massif, Naxos Basal Unit) are all consisting of continental crustal units overlain by shallow-marine carbonate successions. All three units are associated with a crystalline basement, an underlying crust that is still ~25-35 km thick despite widespread extension, and for none of these units evidence exists that this crust consists of younger accreted nappes. Instead, it appears more likely that this crust still consists of the original pre-orogenic continental crust (Searle and Lamont, 2020; van Hinsbergen et al., 2010; 2016) (Figure 1). However, this crust is no longer attached to its (original) mantle lithosphere that instead appears to have subducted (van Hinsbergen et al., 2010). The Barrovian units and their underlying crust underthrusted at a low angle below the overriding plate, which may consist of previously accreted nappes, in the case of the Naxos Basal Unit and the Menderes nappes, or of oceanic lithosphere of the Central Anatolian Ophiolites in the case of the Kırşehir Massif. Kinematic reconstructions of the orogenic architecture (van Hinsbergen et al., 2020) shows that underthrusting of the Barrovian units below the upper plate was a regional feature: it occurred over 150 km or more across-strike of the reconstructed paleo-trench (Figure 1), so far below the upper plate that it must have been present under the entire forearc. Importantly, in the Aegean and western Anatolian cases, the magmatic arcs remained active during horizontal underthrusting, either stable or migrating in the direction of the trench. For the Kırşehir Massif, arc magmatic plutons intruded the massif within a few Ma after underthrusting, and collectively, the three cases suggest that horizontal underthrusting occurred above a normally (30-70°) dipping slab: a flat slab would have shut off the arc, or led to arc migration inboard (e.g., Kay & Mpodozis, 2002; Humphreys, 2009). During this phase of burial and the long-distance underthrusting, the exposed parts of the Barrovian units reached pressures of no more than ~8-11 kbar but at high temperatures reaching anatexis. Stratigraphic constraints show that this burial and prograde metamorphism occurred within ~10 Ma after arrival of the continental unit at the trench, i.e. within the same period as the HP-LT units elsewhere at the same trench. Finally, and paradoxically, underthrusting and syn-burial metamorphism of the Barrovian units may occur while the upper plate was undergoing extension: Oligocene-middle Miocene underthrusting of the Basal Unit occurred while the northern Aegean region underwent extension, and underthrusting of the Kırşehir Block occurred while there was upper plate oceanic spreading forming the Central Anatolian Ophiolites. This shows that the low-angle underthrusting of the Barrovian Units below the upper plate may occur while there is net divergence between the trench and the upper plate, either by roll-back or the retreat of the upper plate away from a mantle stationary trench, or both (van Hinsbergen and Schmid, 2012).

These contrasting prograde metamorphic and tectonic histories occurred simultaneously, along-strike in the Cretaceous for Kırşehir versus Tavşanlı and the Eocene for the Menderes Massif vs. the Cycladic Blueschist, and across-strike in the Oligocene-early Miocene for the Naxos Basal Unit and the Phyllite-Quartzite Unit. To explain these contrasting histories, and the paradox of upper plate extension simultaneously with low-angle underthrusting of continental crust below the entire forearc over 150 km away from the paleo-trench (Figure 1), we propose that the prograde Barrovian metamorphic units may be explained by a scenario of syn-subduction delamination of the downgoing plate that we here refer to as 'lithospheric unzipping' (Figure 3).

Most continent-derived nappes, including those that underwent HP-LT metamorphism, consist of only the sedimentary cover with occasional basement relics, showing that the original continental crystalline crust and mantle lithospheric underpinnings can be dragged down into subduction zones (Handy et al., 2010; Jolivet and Brun, 2010; van Hinsbergen et al., 2005a). The sedimentary facies of the HP-LT metamorphic nappes in the eastern Mediterranean show deep-marine facies and reconstruction places them at microcontinental margins (Tavşanlı, Afyon zones, PQ) or in grabens between horsts (CBS), suggesting that the original underlying continental crust was thinned. We postulate that when thicker continental crust enters the trench during continental subduction, such that its buoyancy resists subduction and/or its strength resists bending, it will no longer be dragged down into the subduction zone, yet it will not stop lithospheric subduction either. Instead, a much thicker section of crust is accreted. In the case of the eastern Mediterranean examples, the underplated crust is still up to 35 km thick, which provides a maximum constraint for the original crustal thickness depending on the amount of shortening and thickening that occurred during or after underthrusting. All three examples of the Kırşehir Block, the Menderes Massif, and the Basal Unit, contain shallow marine platform carbonates suggesting that their original crustal thickness exceeded that of the HP-LT metamorphic units, which show more distal and pelagic-oceanic protoliths.

With the lithospheric unzipping concept (not to be confused with a vertical shear zone system during continental rifting that was also referred to as 'unzipping' by Molnar et al. (2018)), we postulate that instead, a crustal section decouples far below the basement-sediment interface, such that a much thicker crustal section accretes to the upper plate and escapes subduction. In principle, any more or less horizontal weakness zone would be a candidate, but given the crustal thicknesses of the Kırşehir Block, the Menderes Massif, and the Basal Unit, we postulate that the lithospheric mantle decouples along a horizontal decollement around Moho depth during descent. A decoupling between a quartz-dominated middle crust and a mafic lower crust is also plausible. This decoupling horizon forms a subhorizontal tear that propagates into the downgoing plate as its subduction continues (Figure 3), progressively and diachronically ‘unzipping’ the crust from its underlying mantle lithosphere as continental crust is entering the subduction zone. The accreting crust with its much greater thickness than a typical HP-LT nappe maintains a greater strength and coherence, and as long as it is not fully decoupled from the downgoing plate, it will experience 'slab push' that drives it below the overriding plate. The rate at which it underthrusts is the subduction rate minus the shortening rate in the unzipped continental crust.

Because the accreting continental crust is buoyant, it is pushed between the base of the upper plate lithosphere and the underlying mantle wedge, at a low angle (Figure 3). In the case of an accretionary orogen such as in western Turkey and Greece, this upper plate lithosphere consists only of a pile of accreted supracrustal nappes, many of which experienced HP-LT metamorphism, that were stripped from their pre-orogenic crystalline crustal and mantle lithospheric underpinnings. Such orogens thus do not have thick mantle lithosphere as it takes time for lithospheric mantle to re-grow through cooling, and these nappes (e.g., Cycladic

Blueschist Unit, Dilek Nappe, and overlying Afyon and Tavşanlı zones) are thus in direct thrust contact with the underthrusted unzipped crust. In the case of the Kırşehir massif, there were no previously accreted nappes and underthrusting occurred below a thin veneer of subducted oceanic lithosphere-derived subduction mélange and the overlying mantle rocks of the Central Anatolian Ophiolites.

This process of decoupling may utilize the same rheological contrast that permits delamination by peeling mantle lithosphere from a plate (Göğüş and Pysklywec, 2008; Memiş et al., 2020). Such peeling delamination is known to occur at within-plate settings (Göğüş and Ueda, 2018), at former subduction zones where plate convergence has stopped (Göğüş et al., 2011), such as in the SE Carpathians and in the Antalya region (Göğüş et al., 2016; McPhee et al., 2019), and subducting slabs may trigger delamination of lithosphere at slab edges (Spakman and Hall, 2010; van de Lagemaat et al., 2021).

Because the underthrusting crust unzipped from the original mantle lithosphere and is pushed between the hot mantle wedge and the base of the upper plate, it becomes quickly heated from below (in our case studies within 10 Ma after subduction), i.e. at time scales that are much shorter than conductive relaxation of isotherms following crustal thickening (typically 10's Ma; (England and Thompson, 1984; Lamont et al., 2023b) while its positive buoyancy relative to mantle prevents it from sinking. This may explain the rapid HT-MP 'Barrovian' metamorphism during burial. At the same time, subduction of lithospheric mantle continues as a coherent slab. This lithospheric mantle slab continues to hydrate the overlying asthenospheric mantle wedge and if the low-angle underthrusting, unzipped crust reaches the position of the volcanic arc, it may become intruded by arc magmas. In our case studies, where subduction rates were on the order of 2-4 cm/y (van Hinsbergen et al., 2020), and with an arc-trench distance of ~150-200 km (Figure 1), the position of the arc may be reached within 4-10 Ma after entering the subduction zone, but with higher subduction rates, this time gap may be even shorter. Moreover, if there is divergence between the slab and upper plate, because of slab roll-back or upper plate retreat, low-angle underthrusting of unzipping crust may still occur, as it is entirely driven by the slab pull force during subduction of the downgoing plate (Figure 3). This explains the apparent paradox of upper plate extension during continental crustal underthrusting below the extending forearc, as shown for the Cretaceous Central Anatolian and Oligocene-early Miocene Aegean examples. Notably, in western Turkey and Greece, the unzipping occurs after a period of accretion of the only sedimentary cover units (~85-45 Ma in western Turkey, ~70-25 Ma in western Greece), whereby the (thinned) crystalline continental crust and lithosphere were subducted (Jolivet and Brun, 2010; van Hinsbergen et al., 2005a; 2010). However, when the entire continental crust is accreted through unzipping, the subducting lithosphere only consists of dense, cool but entirely ductile lithospheric mantle rocks with a lesser resistance to bending than a thicker full lithospheric section with a strong brittle carapace. We speculate that this may accelerate or initiates subduction hinge retreat during unzipping and continental crustal underplating. This may explain why the Mediterranean region has widespread upper plate extension despite continental subduction (van Hinsbergen and Schouten, 2021; van Hinsbergen et al., 2020). Finally, the underthrusting of a buoyant crust without its dense underpinnings may cause uplift or shorten the forearc even if the trench and upper plate diverge. In the three cases discussed in this paper, this is not straightforwardly tested: there is a sparse stratigraphic oceanic record and no detailed bathymetric estimate of the Central Anatolian ophiolites. It is possible that such uplift was recorded in the forearcs of western Turkey (in the Lycian Nappes) and Greece (e.g., in the Mesohellenic Basin), but future detailed bathymetric analysis is needed to evaluate this.

### *3.2 Region-specific complexities during unzipping*

We argue that the lithospheric unzipping concept explains the shared characteristics of the three cases that we discussed in this paper, but each also has region-specific additional complexities. We will discuss here how and whether they may be reconciled with the unzipping hypothesis, and whether it provides a better explanation than previous interpretations.

The lack of high-pressure metamorphism and the Barrovian conditions in the Menderes Massif shortly after underthrusting were previously explained by delamination, whereby the lithosphere would have gradually peeled back from north to south (van Hinsbergen et al., 2010), as in the numerical experiments of Göğüş and Pysklywec (2008) and Memiş et al. (2020). However, in that concept, low-angle, large-distance underthrusting should have involved the entire downgoing plate, requiring flat slab advance and subsequent rollback of the mantle lithosphere. This hypothesis has difficulty explaining why in Eocene and Oligocene time, shortly after accretion of the nappes, there was arc magmatism only tens of kms north of the Menderes massif. Moreover, the gradual peeling back of lithosphere is a process in which there is no plate boundary, and without net plate convergence (Göğüş and Ueda, 2018; McPhee et al., 2019), whereas Africa-Europe convergence has been continuous. With the lithospheric unzipping hypothesis, subduction may have continued with a single, mantle-stationary or slowly retreating slab during accretion such that arc-trench distances remained stable, and the unzipped crust was underthrust far below the accretionary orogen in the upper plate (Figure 4). In western Anatolia, this underthrusting continued until all continental lithosphere was consumed, after which oceanic subduction resumed, about 35 Ma ago (van Hinsbergen et al., 2010). This unzipped crust underlies much of western Turkey, from the Menderes Massif to the Bey Dağları platform of southwestern Turkey (van Hinsbergen et al., 2010).

An interesting observation in the Menderes Massif is the apparent inverted metamorphic gradient in the nappe stack. First, this requires that shortening occurred in the downgoing crust during burial (Gessner et al., 2001), which is not surprising. However, it also shows that the originally northernmost part of the Menderes Massif that was the first to underthrust and now forms the highest structural unit, experienced the hottest syn-burial conditions, whereas the structurally deeper unit, which consists of sedimentary rocks that only just predated underthrusting and that are still shielded from the mantle by a thick crust al section, experienced lower-temperature conditions. This may reflect the southward increasing depth of the ramp in the decollement as it steps down from the base of the sedimentary cover below the Ören nappe that overlies the Massif, to the Moho below the deepest unit, and largest volume of the Menderes Massif. Where the decollement was shallower, the syn-burial metamorphism occurs at higher temperature and as it gets deeper southward, the temperature decreases. Subsequent thrusting explains the apparent inverted metamorphism.

Previous hypotheses to explain the high-temperature metamorphism in the Kırşehir Massif suggested delamination or slab break-off as heat source (Kadıoğlu et al., 2003; Ilbeyli and Kibici, 2009; Köksal et al., 2012). Alternatively, because the reconstructed trench orientation at which the Kırşehir Massif was N-S and the angle of underthrusting was NNE-SSW, obliquity of subduction was postulated to cause elevated prograde geothermal gradients (van Hinsbergen et al., 2016). Later, numerical experiments showed that obliquity decreases burial rates and therefore allows for higher geothermal gradients during burial (Plunder et al., 2018). However, while these hypotheses may explain part of the observations, they do not explain why the Kırşehir Massif underthrusted ~175 km below the upper plate, followed within a few Ma by the intrusion of arc plutons, and with the upper plate in extension during underthrusting.

The unzipping hypothesis straightforwardly explains the large distance of underthrusting of the Kırşehir Block, towards the position of the arc by 85 Ma, by which time the block had already undergone Barrovian metamorphism and pervasive shearing (Figure 5). Because the Kırşehir block would have remained connected to the downgoing slab during underthrusting, its underthrusting direction was NNE-SSW consistent with syn-metamorphic stretching lineations (Lefebvre, 2011; van Hinsbergen et al., 2016). Upper plate extension, instead, both in the ophiolites (van Hinsbergen et al., 2016), as well as post-accretionary extension that exhumed the Kırşehir massif and surrounding metamorphic massifs (Gürer et al., 2018; Lefebvre et al., 2013) was E-W directed, i.e. at high angles to the subduction direction but perpendicular to the slab that rolled back westwards (Maffione et al., 2017; van Hinsbergen et al., 2020). These two deformation directions reflect the difference between relative plate convergence, and the relative motion between the trench that here was retreating from the overriding plate (Figure 5).

Finally, the complexity of the Oligocene-early Miocene of the Aegean region is that the HP-LT metamorphism of the PQ-Plattenkalk tandem occurs simultaneously with, and to the south of the Barrovian metamorphism of the Naxos Basal Unit. This requires that the two units underthrusted synchronously, the Barrovian Naxos Basal Unit north, and in front of, the PQ and Plattenkalk units (Figure 6). A previous explanation for this contrast invoked that the underthrusting of the Naxos Basal Unit occurred around the same time as the Cycladic Blueschist Unit, after which slab break-off occurred, the Naxos Basal Unit gradually heated up due to crustal thickening, and that renewed subduction to the south caused the formation of the Phyllite-Quartzite unit (Searle and Lamont, 2020). However, seismic tomographic images of the slab below the Aegean region give no reason to infer more than one subducted slab was formed during Aegean orogenesis in the Cenozoic (Faccenna et al., 2003; van Hinsbergen et al., 2005a). Moreover, stratigraphic data show that the Basal Unit correlates to the Tripolitza unit and that the PQ represents the Tripolitza's stratigraphic underpinnings, and that these collectively underthrusted in Oligocene to earliest Miocene time, i.e. long after the underthrusting of the

Cycladic Blueschist unit (Schmid et al., 2020 and references therein). Moreover, geochronological data show that the Basal Unit and PQ reached peak metamorphic conditions (except for younger overprints around granitoids) simultaneously, around 20 Ma (Ring et al., 2001; Jolivet et al., 2010b; Lamont et al., 2020c; 2023b). Hence, we envisage that the underthrusting of the Basal Unit and the PQ/Plattenkalk tandem occurred simultaneously and in-sequence (Figure 6).

The high-temperature metamorphism in the Central Aegean region was previously hypothesized to result from mantle flow around a slab tear (Jolivet et al., 2015) that is imaged with seismic tomography below the SE Aegean region (van Hinsbergen, 2010). If that tear was to explain the syn-burial metamorphism of the Naxos Basal Unit, it should already have existed ~20 Ma ago. Since that time, there has been 200 km of ~N-S plate convergence, and at the longitude of the southeast Aegean region, ~200 km of ~N-S extension as shown by plate kinematic and orogenic deformation reconstruction (van Hinsbergen and Schmid, 2012). Therefore, if a tear would have existed 20 Ma ago, it should have been subducted since and now be several hundred kilometers down into the mantle. Instead, the tear imaged by seismic tomography is right below the lithosphere in southeastern Greece. It must thus be much younger than the early Miocene and cannot have contributed to early Miocene high-T metamorphism. In addition, the magmatic evidence that is thought indicative for a slab tear is based on the occurrence of lamprophyres and high-K magmatism. This did not commence on Kos until ca. 8 Ma and the Western Menderes until ca. 15 Ma (Soder et al. 2016; Fischer et al. 2022). Because this is in a different location and different time to peak Barrovian metamorphism on Naxos (ca. 20-16 Ma), it makes a slab tear an unlikely driver of Barrovian heating in the Cyclades.

We thus postulate that the major horizontal distance of underthrusting of the Basal Unit, and the syn-burial Barrovian metamorphism may be explained by lithospheric unzipping. The structural and stratigraphic evidence for simultaneous underthrusting of the Tripolitza and Ionian nappes from the western Hellenic foreland shows that there was sufficient coupling across the thrust separating these two nappes to keep drive the Tripolitza/Basal unit below the overriding plate until the earliest Miocene (Sotiropoulos et al., 2003; van Hinsbergen and Schmid, 2012). The unzipping of the Tripolitza Platform/Basal Unit crust occurred while the platform was for a large part still in a foreland basin position, similarly to the Bey Dağları platform of southwest

Turkey (Figure 1). This coupling would have allowed the unzipped Tripolitza crust/Basal Unit to underthrust the orogen at low angle, while the Ionian Zone dipped steeper into the mantle behind the unzipped Tripolitza crust. We tentatively infer that the thrust responsible for burial of the Ionian Zone stepped up through the stratigraphy below the adjacent Tripolita Platform, such that the PQ stratigraphic underpinnings of the Tripolitza Platform were buried as part of the Ionian nappe (Figure 6). When coupling across the Tripolitza thrust was lost, slab push was lost and the platform crust accreted to the upper plate. The geochronological evidence suggests that this occurred around 20 Ma or a few million years later (Ring et al., 2001; Jolivet et al., 2010b; Lamont et al., 2020c; 2023b). That there was no longer coupling from that time onwards between the slab and the Tripolitza Platform/Basal Unit is illustrated by the cooling and exhumation of the Phyllite Quarzite Unit of Crete and the Peloponnesos sometime between ~20 Ma and 15 Ma onwards that follows from $^{40}Ar/^{39}Ar$ and fission track cooling data (Jolivet et al., 1996; 2010; Thomson et al., 1998; 1999; Marsellos et al., 2010). This occurred likely by reactivation of the thrust along it was buried, bringing it back up against non-metamorphic the Tripolitza Platform carbonates, while being underthrusted by more external parts of the Ionian zone that are preserved as the Plattenkalk Unit (Jolivet et al., 1996). With this regional modification the unzipping hypothesis may thus explain how two nappes simultaneously formed in sequence, in the same orogen, under contrasting metamorphic conditions, and during roll-back that extended the upper plate (Figure 6).

Finally, it is interesting that whereas the pressures in the Basal Unit in the different parts of the Cyclades are rather uniform (~8-10 kbar on Evvia and Samos, 10-11 kbar on Naxos), temperatures vary quite strongly. The lower pressure units, which represent the shallower sedimentary units, reached temperatures of some 350-400°C (e.g., Ring et al., 2007a), whereas the deeper crystalline basement units on Naxos reached ~700°C (Lamont et al., 2020c). Like for the Menderes, we postulate that this may relate to the lateral thickness variations of the accreting crust due to the southward downstepping decollement, differences in advection of heat possibly by rapid overthrusting, and a greater depth of exhumation of the Naxos Basal Unit, but as for the Menderes Massif, future modelling research may shed further light on the possible thermal responses to our hypothesized lithospheric unzipping process.

### *3.3 Nappe accretion versus unzipping versus slab break-off*

The examples above suggest a first-order relationship between the thickness of the subducting continental crust and the style of accretion. It has been well-established that between the ‘default’ modes of, on the one hand, wholesale subduction of oceanic lithosphere and, in the other hand, arrest of subduction upon the arrival of thick, unextended continental lithosphere, there is a mode of subduction of thinned continental crust and underlying mantle lithosphere that is facilitated by the accretion of its buoyant upper crust to the upper plate (Capitanio et al., 2010; Toussaint et al., 2004). This mode is reflected by thin-skinned nappe stacking and associated HP-LT metamorphism (Jolivet et al., 2003; van Hinsbergen et al., 2005a). The unzipping hypothesis adds another step that may be imaged as a downward stepping decollement horizon with an increasing continental crustal thickness (Figure 7). Based on our observations that unzipped crust tends to be overlain by shallow-water sediments, whereas thin-skinned HP-LT nappes tend to contain more deep-marine sediments, we infer that the unzipping occurs when thicker continental crust arrives in the trench. The precise location of this step may vary: if it occurs in thicker crust, it may entrain shallower-water deposits to HP-LT conditions, like happened with the metabauxites in the CBU, than when it occurs in thinner crust. This step down to lower crustal depths forms an intermediate step between thin-skinned nappe accretion and the arrest of continental subduction altogether.

## 4. Unzipping elsewhere and on the Proterozoic Earth?

The metamorphic contrasts that we summarized from the eastern Mediterranean region are not unique. For instance, the Eocene high-temperature metamorphism and anatexis that occurred in rocks of the Himalaya that were accreted to the upper Asian plate when continental crust of the Indian plate arrived at the south Tibetan trench in the Eocene (Hodges, 2000), ~60-55 Ma ago (Hu et al., 2015). Those first continental units to arrive were the Tibetan Himalaya - a sedimentary sequence from Paleozoic to Eocene rocks that mostly escaped metamorphism (Jadoul et al., 1998) - and the Greater Himalaya, consisting of mostly Precambrian basement and sediments that are traced over ~1500 km of the Himalayan orogen. The Greater Himalaya escaped HP-LT metamorphism (Stübner et al., 2014) but instead underwent HT/MP (730-775°C / 10-13 kbar (Corrie and Kohn, 2011; Khanal et al., 2021)). This metamorphism was underway by 50 Ma and continuing throughout the Eocene (Khanal et al., 2021; Smit et al., 2014) and anatexis, producing leucogranites within ~10 Ma after their incorporation in the Himalayan orogen (e.g., Cao et al., 2022). In contrast, rocks of the northwestern Tethyan/Greater Himalayan continental margin underwent UHP-LT (22-23 kbar, 400-425°C) metamorphism starting around 57 Ma and HP/LT conditions prevailing until ~47 Ma (Chatterjee and Jagoutz, 2015; de Sigoyer et al., 2000; Guillot et al., 2008; Leech et al., 2005; Palin et al., 2017), i.e. simultaneously with the HT/MP conditions along the Greater Himalayan rocks to the east. Interestingly, Bird (1978) already suggested that the HT conditions in the Greater Himalaya may be explained by delamination of the Indian Plate during underthrusting – equivalent to our unzipping hypothesis. Combined with the (U)HP-LT metamorphism of the Tso Morari complex in the far northwestern corner of the Tethyan Himalaya, this pair may be equivalent to, albeit at a larger scale, rge Menderes and Cycladic Blueschist contrast (Figure 4): the western, thinned margin of the Tethyan/Greater Himalaya was dragged down into the subduction zone, whereas the thicker crust unzipped, underthrusted, and became juxtaposed with the mantle wedge, and heated up. Only much later, in Miocene time, was the high-temperature Greater Himalaya crust exhumed by extrusion (e.g., Beaumont et al., 2001).

The lithospheric unzipper hypothesis may also explain Barrovian conditions in the deep parts of accretionary Phanerozoic orogens elsewhere. For instance, we postulate that the rapid Barrovian conditions reached by the Venidiger Nappe in the heart of the Tauern Window may record the unzipping of downgoing Eurasian lithosphere. The Venidiger Nappe is the lowermost structural unit and the youngest nappe of the eastern Alps. It not only contains sedimentary cover units but also underlying Paleozoic basement of the Eurasian Variscan belt, it escaped HP-LT metamorphism and instead underwent MP-HT Barrovian metamorphism (9-13 kbar, 550°C), <6 Ma after the overlying thin-skinned thrust slices reached peak (U)HP-LT metamorphic conditions (Smye et al., 2011; Schmid et al., 2013). In both the Alps and Himalaya, the architecture and sequence of tectonic and metamorphic events bear resemblance that of the eastern Mediterranean examples and may potentially be explained by the unzipping hypothesis.

Previous concepts of nappe accretion and associated HP-LT metamorphism reconciled the apparent jumps in subduction thrusts in geological records of orogens that appear as jumping subduction zones with the activity of a single subduction zone that consumed oceanic and continental lithosphere (Handy et al., 2010; Jolivet and Brun, 2010; Tirel et al., 2013; van Hinsbergen et al., 2005a). This satisfied the geophysical observations that show a continuous slab at depth below these orogens. The unzipping hypothesis may now also reconcile the presence of hot Barrovian continental units that escaped HP-LT metamorphism in those orogens with a continuous process of shallow angle (continental) subduction.

This may offer a geodynamic scenario that could explain the formation of hot Proterozoic orogens in context of subduction. For instance, the Paleoproterozoic Trans-Hudson orogen of North-America (Figure 8), a deeply eroded accretionary orogen (Corrigan et al., 2009), is characterized by the abundance of accreted, thick continental crystalline basement with only rare supracrustal nappes. These units do not reveal evidence of early orogenic HP-UHP metamorphism but display predominantly Barrovian metamorphism that commonly reaches granulites facies temperatures but rarely reaches pressures above 8-10 kbar. These conditions overlap with or predating arc magmatism, and even though the continental fragments that constitute the orogen have markedly different geological histories and are interpreted to represent individual microcontinent, there is a near total absence of ophiolites or oceanic material between these accreted terranes (Corrigan et al., 2009; Godet et al., 2021; St-Onge et al., 2006; Weller et al., 2013 and references therein). More specifically, the South-East Churchill Province branch (Corrigan et al., 2018; Godet et al., 2021; Wardle et al., 2002) of the Trans-Hudson Orogen (Figure 8) is comprised of upper amphibolite to granulite facies crystalline basement units of 50-100 km wide, the Core Zone, separating the lower plate Superior craton and its rifted margin volcanic-sedimentary sequences (the Labrador Trough) from the upper plate North Atlantic Craton (Figure 8). Arc magmatism swept across the core zone from the upper plate towards the lower plate, always predated by Barrovian metamorphism (Godet et al., 2021). Maximum pressures recorded were on the order of 11 kbar for granulite facies rocks (Charette et al., 2021; Godet et al., 2021), with a preserved Barrovian sequence on the western edge of the orogen (Godet et al., 2020).

Several long-lived crustal-scale anastomosing shear zones within the Core Zone separate continental blocks of contrasting isotopic signatures, leading authors to interpret them as microcontinents with each shear zone representing individual suture zones (Corrigan et al., 2018; 2021), i.e. former subduction zones that must have consumed oceanic lithosphere by wholesale subduction, leading to an absence of oceanic exotic material in between the continental fragments. The sweeping of arc magmatism is thus implicitly seen as individual arcs birthing and dying as small ocean basins sequentially subduct and close between the terranes, with separate subduction initiation events within each basin, and multiple slabs involved (e.g., Corrigan et al., 2018; 2021; Wardle et al., 2002). However, Godet et al. (2021), in their regional magmatic and metamorphic compilation, already noted that the orogenic architecture is not as expected for a modern accretionary orogen that formed in such a fashion such as Mesozoic-Cenozoic Tibet (Kapp and DeCelles, 2019), noting the absence of oceanic material or (U)HP-LT metamorphism, and the rapid development and duration of granulite conditions directly after accretion and even before the arrival of arc magmatism. We propose that such characteristics may be well explained by successive accretion of pericratonic microcontinents through lithospheric unzipping (Figure 8). Such an explanation requires only one eastward-dipping slab (present-day coordinates) that subducted over the 150 Myrs evolution of the South-East Churchill Province, as previously postulated by Godet (2020). We postulate that the decollement horizon coincided with the top of the crust in the oceanic basins and stepped down to the Moho in the intervening microcontinents. This then led to successive accretion through lithospheric unzipping of Superior affinity peri-cratonic blocks to the North Atlantic Craton accompanied by slab roll-back relative to that craton left the upper plate without a thick lithospheric mantle, providing an explanation for the widespread lower-plate-ward sweeping of granulite facies metamorphic conditions closely followed by arc magmatism, and for penetrative deformation and coeval anastomosed shear zone development all throughout the Province.

If in a hotter Earth, the Moho was weaker and more prone to becoming the decollement horizon than the sediment-basement interface, lithospheric unzipping may have been the rule rather than the exception. This mode of orogenesis may have been the default until continents became strong enough so that their thinned margins became dragged down into subduction zones. This transition may have occurred at around 650 Ma, when metamorphic, geochemical, and plate tectonic lines of evidence suggest that deep continental recycling into the mantle initiated (Brown and Johnson, 2018; Brown et al., 2022; Jackson and Macdonald, 2022). The lithospheric unzipper concept may thus explain hot Proterozoic orogenesis as a geological expression of modern-style (continental) subduction in an Earth that was much hotter than today.

## 5. Conclusions

Phanerozoic accretionary orogens typically consist of thin-skinned, upper crustal nappes that were offscraped from subducted oceanic or continental lithosphere that, where sufficiently buried, display (ultra) high-pressure, low-temperature (U)HP-LT metamorphism. These are straightforwardly explained by the progressive, episodic decoupling of upper crustal units during ongoing subduction, whereby the typical cold metamorphism is explained by burial and exhumation of nappes along the plate interface. Surprisingly, however, the deepest continental structural units of accretionary mountain belts often escaped HP-LT metamorphism and underwent prograde, 'Barrovian' MP-HT metamorphism instead.

Here we review three of these enigmatic Barrovian complexes in the eastern Mediterranean region and compare each of these to time-equivalent HP-LT metamorphic nappes that formed laterally at the same subduction zone. These include the Barrovian Kırşehir Block, Menderes Massif, and Naxos-Samos Basal Unit, which formed simultaneously with the HP-LT metamorphic Tavşanlı zone, Cycladic Blueschist, and Phyllite-Quartzite/Plattenkalk units. We conclude that the continental units that underwent prograde Barrovian metamorphism underthrusted at low angle below the forearc over distances of up to 150 km or more, likely still contain the entire pre-orogenic continental crust but not their mantle lithosphere and reached close to or even beyond the location of the magmatic arc that intruded the unit after accretion.

We postulate that this major horizontal underthrusting is the result of a process of gradual 'unzipping' of the low-angle underthrusting crust from the steeply subducting slab. The underthrusting crust penetrates between the upper plate lithosphere (which in accretionary orogens, or below oceanic forearcs with supra-subduction zone spreading centers is typically very thin) and the underlying mantle wedge. Unprotected by its decoupled and subducting mantle lithospheric underpinnings, the underthrusted crust undergoes high-temperature metamorphism and pervasive shearing. The process of lithospheric unzipping in the eastern Mediterranean orogens likely forms an intermediate stage between steep continental margin subduction and thin-skinned nappe accretion, and the arrest of subduction upon arrival of thick, unstretched continent.

Finally, we propose that in a hotter, Proterozoic Earth, the process of unzipping may have been the default response of continents to subduction, making enigmatic hot orogenesis characteristics for Proterozoic orogens, such as in the Trans-Hudson orogen of Canada, possible geological expressions of modern-style continental subduction in a hotter Earth.

**Acknowledgements**

DJJvH acknowledges NWO Vici grant 865.17.001. CG acknowledges NSERC funding (grant RGPIN-2020-06400). We thank Vincent Roche, Oğus Göğüş, Uwe Ring, and Joel Saylor for reviews.

**Open Research**

No new codes or data were used for this paper.

**Figure 1**: A) Tectonic map of the Aegean and Anatolian regions, with the modern and restored positions of the synchronous nappes with contrasting thermal evolutions. B, C, D) Paleo-tectonic reconstructions, based on (van Hinsbergen et al., 2020), showing the paleogeographic positions during underthrusting of the Phyllite-Quartzite/Plattenkalk vs. Basal Unit, Cyclading Blueschist Unit versus Menderes Massif, and the Tavşanlı Zone vs Kırşehir Block, respectively. AZ = Afyon Zone; BD = Bey Dağları platform; BU = Basal Unit; CAO = Central Anatolian Ophiolites; CBU = Cycladic Blueschist Unit; Ev = Evvia; Io = Ionian Nappe; KB = Kırşehir Block; LN = Lycian Nappes; MB = Mesohellenic Basin; MM = Menderes Massif; Na = Naxos; NAFZ = North Anatolian Fault Zone; Ol = Mt. Olympos; Os = Mt. Ossa; Pi = Pindos Nappe; PQ/PK = Phyllite-Quartzite/Plattenkalk units; Sa = Samos; SaS =. Sava Suture Zone; Tr = Tripolitza Nappe; TZ = Tavşanlı Zone. B, C, D) Tectonic reconstructions at 20, 45, and 85 Ma, corresponding to the timing of underthrusting of the Phyllite-Quartzite/Plattenkalk and Basal Unit, Cyclading Blueschist Unit and Menderes Massif, and Tavşanlı Zone and Kırşehir Block, respectively. E, F, G) lithospheric cross-sections across the Aegean, west Anatolian, and central Anatolian orogenic segments, respectively. Sections A-A' is modified from Schmid et al. (2020): those authors presumed that the crust underlying all of the Aegean orogen from the Sava Suture Zone to the south was underlain by Ionian Nappe continental crust. The steep subduction of the Phlyllite-Quartzite/Plattenkalk units found in the Aegean forearc of Crete and the Peloponnesos precludes this, and instead, we here interpret the Aegean crust north of Crete to be underlain by Naxos Basal Unit/Tripolitza crust. Section B-B' is modified from van Hinsbergen et al. (2010) and Schmid et al. (2020). Section C-C' is modified from van McPhee et al. (2022).

**Figure 2**: Compilation of P-T-t paths and estimates of peak metamorphic conditions for HP-LT nappes and MP-HT nappes for the three case study areas. HP-LT nappes include: the Tavsanli Zone (green), 24 kbar, 500°C (Davis and Whitney, 2008; Okay, 2002; Plunder et al., 2013). Lu/Hf geochronology on garnet and lawsonite between ~91-83 Ma (Mulcahy et al., 2014; Pourteau et al., 2019). Cycladic Blueschist Unit (dark blue), 18-23 kbar, 500-600°C and U/Pb zircon and allanite and Lu/Hf garnet ages between ~55-38 Ma (Behr et al., 2018; Lamont et al., 2020b; Laurent et al., 2017; Skelton et al., 2019; Wolfe et al., 2023). Phyllite Quartzite Unit

(light blue) 18 kbar 400°C dated at ~24-20 Ma by Ar-Ar (Jolivet et al., 1996; 2010b). MP-HT nappes that are coeval with HP-LT nappes include: the Kırşehir Massif (orange) 5-8 kbar, 700°C (Lefebvre et al., 2015; Whitney and Dilek, 1998; Whitney and Hamilton, 2004; Whitney et al., 2003), dated at ~90-85 Ma by U-Pb monazite and zircon (Whitney and Hamilton, 2004; Whitney et al., 2003). Menderes Massif (yellow) 6-8 kbar and 500-550°C (Okay, 2001; Whitney and Bozkurt, 2002), at ~42 and 35 Ma dated by Lu/Hf on garnet (Schmidt et al., 2015), Rb-Sr (Bozkurt et al., 2011) and 40Ar-39Ar syn-metamorphic ages of greenschists (Lips et al., 2001). Naxos Basal Unit (red) ~10-11 kbar and ~600-730°C, dated by U-Pb zircon at 20-16 Ma (Keay and Lister, 2002; Lamont et al., 2020c; 2023b)

**Figure 3**: The lithospheric unzipper concept versus deep underthrusting and nappe stacking. During lithospheric unzippin, the decollement steps down from to Moho depths, and the buoyant downgoing plate’s crust underthrusts the upper plate at low angle while the mantle lithosphere subducts steeply.

**Figure 4**. 3D cartoon showing the contrasting deep subduction and nappe stacking of the Cycladic Blueschist Unit versus lithospheric unzipping and low-angle underthrusting of the Menderes Massif. For key to inset map, see Figure 1.

**Figure 5**. 3D cartoon showing the contrasting deep subduction and nappe stacking of the Tavşanlı zone, versus lithospheric unzipping and low-angle underthrusting of the Kırşehir Block at nearly perpendicular trenches. For key to inset map, see Figure 1.

**Figure 6**. 2D cross sections showing the simultaneous underthrusting of the unzipped, low-angle underthrusting Basal Unit and the steeply subducting Phyllite-Quartzite and Plattenkalk units. These processes occurred during roll-back, below an extending upper plate. For key to inset map, see Figure 1.

**Figure 7**. Four stages of subduction as a function of the down-stepping of a decollement through a continental lithosphere, from whole-sale subduction with a decollement coinciding with the top of the sediment pile, to nappe stacking when the decollement steps down to the sediment-basement interface, to unzipping when the decollement steps down to the base of the crust, to slab break-off when the decollement steps down to the base of the lithosphere.

**Figure 8**. A) Tectonic map of the Trans-Hudson orogen and the South-East Churchill province, modified after Corrigan et al. (2021); B) Cross-section of the accreted continental crustal fragments of the Core Zone of the South-East Churchill Province modified after Corrigan et al. (2021); C) schematic diagram illustrating the decollement location in a conceptual pre-orogenic cross section. If the decollement horizon coincided with the Moho of the microcontinental fragments such that they unzipped during continental subduction, and with the top of the crust of intervening oceanic basins, the juxtaposition of the continents without intervening accretionary prisms, and their westward sweeping Barrovian metamorphism trailed by arc magmatism may be explained by the continuous subduction of a single slab. See text for further discussion.

## 1. References

Abgarmi, B., Delph, J. R., Ozacar, A. A., Beck, S. L., Zandt, G., Sandvol, E., et al. (2017). Structure of the crust and African slab beneath the central Anatolian plateau from receiver functions: New insights on isostatic compensation and slab dynamics. *Geosphere, 13*(6), 1774-1787.

Advokaat, E. L., van Hinsbergen, D. J. J., Kaymakcı, N., Vissers, R. L. M., & Hendriks, B. W. H. (2014). Late Cretaceous extension and Palaeogene rotation-related contraction in Central Anatolia recorded in the Ayhan-Büyükkışla basin. *International Geology Review, 56*(15), 1813-1836.

Akay, E. (2009). Geology and petrology of the Simav Magmatic Complex (NW Anatolia) and its comparison with the Oligo-Miocene granitoids in NW Anatolia: implications on Tertiary tectonic evolution of the region. *International Journal of Earth Sciences, 98,* 1655-1675.

Altherr, R., Kreuzer, H., Wendt, I., Lenz, H., Wagner, G.A. & Keller, J. (1982). A late Oligocene/early Miocene high temperature belt in the Attic-Cycladic crystalline complex (SE Pelagonian, Greece). *Geologisches Jahrbuch. Reihe E, Geophysik 23*, 97-164.

Altherr, R., Henjes-Kunst, F., Matthews, A., Friedrichsen, H., & Hansen, B. T. (1988). O-Sr istotopic variations in Miocene granitoids from the Aegean: Evidence for an origin by combined assimilation and fractional crystallisation. *Contributions to Mineralogy and Petrology, 100*, 528-541.

Barazangi, M., Sandvol, E., & Seber, D. (2006). Structure and tectonic evolution of the Anatolian plateau in eastern Turkey. *Geological Society of America Special Paper, 409*, 463-473.

Beaumont, C., Jamieson, R.A., Nguyen, M.H., & Lee, B. (2001). Himalayan tectonics explained by extrusion of a low-viscosity crustal channel coupled to focused surface denudation. *Nature, 414*, 738-742.

Behr, W. M., Kotowski, A. J., & Ashley, K. T. (2018). Dehydration-induced rheological heterogeneity and the deep tremor source in warm subduction zones. *Geology, 46*(5), 475-478.

Berk Biryol, C., Beck, S. L., Zandt, G., & Özacar, A. A. (2011). Segmented African lithosphere beneath the Anatolian region inferred from teleseismic P-wave tomography. *Geophysical Journal International, 184*(3), 1037-1057.

Bird, P. (1978). Initiation of intracontinental subduction in the Himalaya. *Journal of Geophysical Research: Solid Earth, 83(B10)*, 4975-4987.

Blumor, T., Dollinger, J., Mutter, A., Zardam, S., & Kowalczyk, G. (1994). Plattenkalk Series and kastania Phyllites of the Taygetos MTS.: new results on structure and succession. *Δελτίον της Ελληνικής Γεωλογικής Εταιρίας, 30*(2), 83-92.

Bolhar, R., Ring, U. & Ireland, T.R. (2017). Zircon in amphibolites from Naxos, Aegean Sea, Greece: origin, significance and tectonic setting. *Journal of Metamorphic Geology 35*, 413-434.

Bonneau, M. (1984). Correlation of the Hellenide nappes in the south-east Aegean and their tectonic reconstruction. *Geological Society, London, Special Publications 17,* 517-527.

Bozkurt, E., & Oberhänsli, R. (2001). Menderes Massif (Western Turkey): structural, metamorphic and magmatic evolution - a synthesis. *International Journal of Earth Sciences, 89*(4), 679-708.

Bozkurt, E., Satır, M., & Buğdaycıoğlu, Ç. (2011). Surprisingly young Rb/Sr ages from the Simav extensional detachment fault zone, northern Menderes Massif, Turkey. *Journal of Geodynamics, 52*(5), 406-431.

Bröcker, M., & Pidgeon, R. T. (2007). Protolith ages of meta-igneous and metatuffaceous rocks from the Cycladic blueschist unit, Greece: results of a reconnaissance U-Pb zircon study. *The Journal of Geology, 115*(1), 83-98.

Brown, M. (1993). P–T–t evolution of orogenic belts and the causes of regional metamorphism. *Journal of the Geological Society, 150*(2), 227-241.

Brown, M. (2007). Metamorphic conditions in orogenic belts: a record of secular change. *International Geology Review, 49*(3), 193-234.

Brown, M., & Johnson, T. (2018). Secular change in metamorphism and the onset of global plate tectonics. *American Mineralogist, 103*(2), 181-196.

Brown, M., Johnson, T., & Spencer, C. J. (2022). Secular changes in metamorphism and metamorphic cooling rates track the evolving plate-tectonic regime on Earth. *Journal of the Geological Society, 179*(5), jgs2022-2050.

Brun, J.-P., & Faccenna, C. (2008). Exhumation of high-pressure rocks driven by slab rollback. *Earth and Planetary Science Letters, 272*(1-2), 1-7.

Brun, J.-P., & Sokoutis, D. (2007). Kinematics of the Southern Rhodope Core Complex (North Greece). *International Journal of Earth Sciences, 96*(6), 1079-1099.

Brun, J. P., & Sokoutis, D. (2010). 45 m.y. of Aegean crust and mantle flow driven by trench retreat. *Geology, 38*(9), 815-818.

Candan, O., Çetinkaplan, M., Oberhänsli, R., Rimmelé, G., & Akal, C. (2005). Alpine high-P/low-T metamorphism of the Afyon Zone and implications for the metamorphic evolution of Western Anatolia, Turkey. *Lithos, 84*(1-2), 102-124.

Cao, H.-W., Pei, Q.-M., Santosh, M., Li, G.-M., Zhang, L.-K., Zhang, X.-F., Zhang, Y.-H., Zou, H., Dai, Z.-W. and Lin, B. (2022). Himalayan leucogranites: A review of geochemical and isotopic characteristics, timing of formation, genesis, and rare metal mineralization, *Earth-Science Reviews, 104229.*

Capitanio, F. A., Morra, G., Goes, S., Weinberg, R. F., & Moresi, L. (2010). India–Asia convergence driven by the subduction of the Greater Indian continent. *Nature Geoscience, 3*(2), 136-139.

Cawood, P. A., Kröner, A., Collins, W. J., Kusky, T. M., Mooney, W. D., & Windley, B. F. (2009). Accretionary orogens through Earth history. *Geological Society, London, Special Publications, 318*(1), 1-36.

Cenki-Tok, B., Expert, M., Işık, V., Candan, P., Monié, P., & Bruguier, O. (2016). Complete Alpine reworking of the northern Menderes Massif, western Turkey. *International Journal of Earth Sciences 105*, 1507-1524.

Çetinkaplan, M., Candan, O., Oberhänsli, R., Sudo, M. & Cenki-Tok, B., (2020). P–T–t evolution of the Cycladic Blueschist Unit in Western Anatolia/Turkey: Geodynamic implications for the Aegean region. *Journal of Metamorphic Geology 38*, 379-419.

Charette, B., Godet, A., Guilmette, C., Davis, D. W., Vervoort, J., Kendall, B., et al. (2021). Long-lived anatexis in the exhumed middle crust of the Torngat Orogen: Constraints from phase equilibria modeling and garnet, zircon, and monazite geochronology. *Lithos, 388*, 106022.

Chatterjee, N., & Jagoutz, O. (2015). Exhumation of the UHP Tso Morari eclogite as a diapir rising through the mantle wedge. *Contributions to Mineralogy and Petrology*, *169*, 1-20.

Cisneros, M., Barnes, J. D., Behr, W. M., Kotowski, A. J., Stockli, D. F., & Soukis, K. (2021). Insights from elastic thermobarometry into exhumation of high-pressure metamorphic rocks from Syros, Greece. *Solid Earth, 12*(6), 1335-1355.

Collins, A. S., & Robertson, A. H. F. (2003). Kinematic evidence for Late Mesozoic–Miocene emplacement of the Lycian Allochthon over the western Anatolide belt, SW Turkey. *Geological Journal, 38*(3-4), 295-310.

Corrie, S. L., & Kohn, M. J. (2011). Metamorphic history of the central Himalaya, Annapurna region, Nepal, and implications for tectonic models. *Bulletin, 123*(9-10), 1863-1879.

Corrigan, D., Pehrsson, S., Wodicka, N., & De Kemp, E. (2009). The Palaeoproterozoic Trans-Hudson Orogen: a prototype of modern accretionary processes. *Geological Society, London, Special Publications, 327*(1), 457-479.

Corrigan, D., van Rooyen, D., & Wodicka, N. (2021). Indenter tectonics in the Canadian Shield: A case study for Paleoproterozoic lower crust exhumation, orocline development, and lateral extrusion. *Precambrian Research, 355*, 106083.

Corrigan, D., Wodicka, N., McFarlane, C., Lafrance, I., Rooyen, D. v., Bandyayera, D., & Bilodeau, C. (2018). Lithotectonic framework of the core zone, Southeastern Churchill Province, Canada. *Geoscience Canada, 45*(1), 1-24.

Cossette, É., Audet, P., Schneider, D., & Grasemann, B. (2016). Structure and anisotropy of the crust in the Cyclades, Greece, using receiver functions constrained by in situ rock textural data. *Journal of Geophysical Research: Solid Earth, 121*(4), 2661-2678.

Davis, P. B., & Whitney, D. L. (2008). Petrogenesis and structural petrology of high-pressure metabasalt pods, Sivrihisar, Turkey. *Contributions to Mineralogy and Petrology, 156*(2), 217-241.

Delph, J. R., Abgarmi, B., Ward, K.M., Beck, S.L., Özacar, A.A., Zandt, G., Sandvol, E., Türkelli, N. & Kalafat, D. (2017). The effects of subduction termination on the continental lithosphere: Linking volcanism, deformation, surface uplift, and slab tearing in central Anatolia. *Geosphere 13*, 1788-1805.

Dercourt, J., Zonenshain, L.P., Ricou, L.E., Kazmin, V.G., Le Pichon, X., Knipper, A.L., Grandjacquet, C., Sbortshikov, I.M., Geyssant, J. & Lepvrier, C. (1986). Geological evolution of the Tethys belt from the Atlantic to the Pamirs since the Lias. *Tectonophysics 123*, 241-315.

de Sigoyer, J., Chavagnac, V., Blichert-Toft, J., Villa, I. M., Luais, B., Guillot, S., Cosca, M. & Mascle, G. (2000). Dating the Indian continental subduction and collisional thickening in the northwest Himalaya: Multichronology of the Tso Morari eclogites. *Geology, 28*(6), 487-490.

Dilek, Y. & Whitney, D. L. (1997). Counterclockwise PTt trajectory from the metamorphic sole of a Neo-Tethyan ophiolite (Turkey). *Tectonophysics, 280*, 295-310.

Dragovic, B., Samanta, L. M., Baxter, E. F., & Selverstone, J. (2012). Using garnet to constrain the duration and rate of water-releasing metamorphic reactions during subduction: An example from Sifnos, Greece. *Chemical Geology*, *314*, 9-22.

Ducharme, T., Schneider, D.A., Grasemann, B. & Klonowska, I. (2022). Stretched thin: Oligocene extrusion and ductile thinning of the Basal Unit along the Evia Shear Zone, NW Cyclades, Greece. *Tectonics* *41*, e2022TC007561.

Endrun, B., Lebedev, S., Meier, T., Tirel, C., & Friederich, W. (2011). Complex layered deformation within the Aegean crust and mantle revealed by seismic anisotropy. *Nature Geoscience*, *4*(3), 203-207.

England, P. C., & Thompson, A. B. (1984). Pressure—temperature—time paths of regional metamorphism I. Heat transfer during the evolution of regions of thickened continental crust. *Journal of Petrology*, *25*(4), 894-928.

Ersoy, E. Y., & Palmer, M. R. (2013). Eocene-Quaternary magmatic activity in the Aegean: Implications for mantle metasomatism and magma genesis in an evolving orogeny. *Lithos*, *180*, 5-24.

Faccenna, C., Jolivet, L., Piromallo, C., & Morelli, A. (2003). Subduction and the depth of convection in the Mediterranean mantle. *Journal of Geophysical Research: Solid Earth* *108*, doi: 10.1029/2001jb001690.

Fassoulas, C., Kilias, A., & Mountrakis, D. (1994). Postnappe stacking extension and exhumation of high-pressure/low-temperature rocks in the island of Crete, Greece. *Tectonics*, *13*, 127-138.

Feenstra, A. (1985). Metamorphism of bauxites on Naxos, Greece. *Geologica Ultraiectina 39*, 1-206.

Fischer, S., Prelević, D., Akal, C., Romer, R. L., & Gerdes, A. (2022). The Role of Syn-Extensional Lamprophyre Magmatism in Crustal Dynamics—the Case of the Menderes Metamorphic Core Complex, Western Turkey. *Journal of Petrology*, *63*(4), egac024.

Fleury, J. J. & Godfriaux, I. (1974). Arguments pour l'attribution de la série de la fenêtre de l'Olympe (Grece)a la zone de Gavrovo Tripolitza: présence de fossiles du Maastrichtien et de l'Eocene inférieur (et moyen?). *Annales de la Société Géologique du Nord*, *94*, 149-156.

Floyd, P. A., Göncüoğlu, M. C., Winchester, J. A., & Yaliniz, M. K. (2000). Geochemical Character and Tectonic Environment of Neotethyan Ophiolitic Fragments and Metabasites in the Central Anatolian Crystalline Complex, Turkey. *Geological Society, London, Special Publications*, *173*, 183-202.

Gautier, P., Brun, J.P., Moriceau, R., Sokoutis, D. & Jolivet, L. (1999). Timing, kinematics and cause of Aegean extension: a scenario based on a comparison with simple analogue experiments. *Tectonophysics*, *315*, 31-72.

Gautier, P., Bozkurt, E., Bosse, V., Hallot, E. & Dirik, K. (2008). Coeval extensional shearing and lateral underflow during Late Cretaceous core complex development in the Niğde Massif, Central Anatolia, Turkey. *Tectonics*, *27*, doi: 10.1029/2006tc002089

Gessner, K., Gaillardo, L.A., Markwitz, V., Ring, U. & Thomson, S.A. (2013). What caused the denudation of the Menderes Massif: Review of crustal evolution, lithosphere structure, and dynamic topography in southwest Turkey. *Gondwana Research 24*, 243-274.

Gessner, K., Ring, U., & Güngör, T. (2011). Field Guide to Samos and the Menderes Massif: Along-Strike Variations in the Mediterranean Tethyan Orogen. *Geological Society of America Field Guide*, *23*, 1-52.

Gessner, K., Ring, U., Passchier, C. W., & Güngör, T. (2001). How to resist subduction: evidence for large-scale out-of-sequence thrusting during Eocene collision in western Turkey. *Journal of the Geological Society*, *158*(5), 769-784.

Glazner, A. F. & J. M. Bartley (1985). Evolution of lithospheric strength after thrusting. *Geology 13*, 42-45.

Godet, A. (2020). Styles métamorphique et tectonique au Paléoprotérozoïque: Exemple du sud-est de la province du Churchill, Québec, Canada. *PhD Thesis, Université Laval*, 396 pp.

Glodny, J. & U. Ring (2022). The Cycladic Blueschist Unit of the Hellenic subduction orogen: Protracted high-pressure metamorphism, decompression and reimbrication of a diachronous nappe stack. *Earth-Science Reviews 224*, 103883.

Godet, A., Guilmette, C., Labrousse, L., Smit, M. A., Cutts, J. A., Davis, D. W., & Vanier, M. A. (2021). Lu–Hf garnet dating and the timing of collisions: Palaeoproterozoic accretionary tectonics revealed in the Southeastern Churchill Province, Trans-Hudson Orogen, Canada. *Journal of Metamorphic Geology, 39*(8), 977-1007.

Godet, A., Guilmette, C., Labrousse, L., Smit, M. A., Davis, D. W., Raimondo, T., et al. (2020). Contrasting PTt paths reveal a metamorphic discontinuity in the New Quebec Orogen: Insights into Paleoproterozoic orogenic processes. *Precambrian Research*, *342*, 105675.

Göğüş, O. H., & Pysklywec, R. N. (2008). Mantle lithosphere delamination driving plateau uplift and synconvergent extension in eastern Anatolia. *Geology*, *36*(9), 723-726.

Göğüş, O. H., Pysklywec, R.N., Corbi, F. & Faccenna, C. (2011). The surface tectonics of mantle lithosphere delamination following ocean lithosphere subduction: Insights from physical-scaled analogue experiments. *Geochemistry, Geophysics, Geosystems 12*, https://doi.org/10.1029/2010GC003430.

Göğüş, O. H., Pysklywec, R. N., & Faccenna, C. (2016). Postcollisional lithospheric evolution of the Southeast Carpathians: Comparison of geodynamical models and observations. *Tectonics*, *35*(5), 1205-1224.

Göğüş, O. H., & Ueda, K. (2018a). Peeling back the lithosphere: Controlling parameters, surface expressions and the future directions in delamination modeling. *Journal of Geodynamics*, *117*, 21-40.

Gorce, J. S., Caddick, M. J., Baxter, E. F., Dragovic, B., Schumacher, J. C., Bodnar, R. J., & Kendall, J. F. (2021). Insight into the early exhumation of the Cycladic Blueschist Unit, Syros, Greece: Combined application of zoned garnet geochronology, thermodynamic modeling, and quartz elastic barometry. *Geochemistry, Geophysics, Geosystems*, *22*(8), e2021GC009716.

Guillot, S., Mahéo, G., de Sigoyer, J., Hattori, K. H., & Pêcher, A. (2008). Tethyan and Indian subduction viewed from the Himalayan high- to ultrahigh-pressure metamorphic rocks. *Tectonophysics*, *451*(1-4), 225-241.

Guilmette, C., Smit, M.A., van Hinsbergen, D.J.J., Gürer, D., Corfu, F., Charette, B., Maffione, M., Rabeau, O., & Savard, D. (2018). Forced subduction initiation recorded in the sole and crust of the Semail Ophiolite of Oman. *Nature Geoscience*, *11*, 688-695.

Guilmette, C., van Hinsbergen, D.J.J., Smit, M.A., Godet, A., Fournier-Roy, F., Butler, J., Maffione, M., Li, S., & Hodges, K. (2023). Formation of the Xigaze Metamorphic Sole under Tibetan continental lithosphere reveals generic characteristics of subduction initiation. *Communications Earth & Environment*, *4*, 339.

Gülyüz, E., Kaymakci, N., Meijers, M. J. M., van Hinsbergen, D. J. J., Lefebvre, C., Vissers, R. L. M., et al. (2013). Late Eocene evolution of the Çiçekdağı Basin (central Turkey): Syn-sedimentary compression during microcontinent–continent collision in central Anatolia. *Tectonophysics*, *602*, 286-299.

Gürer, D., Plunder, A., Kirst, F., Corfu, F., Schmid, S. M., & van Hinsbergen, D. J. J. (2018). A long-lived Late Cretaceous–early Eocene extensional province in Anatolia? Structural evidence from the Ivriz Detachment, southern central Turkey. *Earth and Planetary Science Letters, 481*, 111-124.

Gürer, D., van Hinsbergen, D. J. J., Matenco, L., Corfu, F., & Cascella, A. (2016). Kinematics of a former oceanic plate of the Neotethys revealed by deformation in the Ulukışla basin (Turkey). *Tectonics*, *35*(10), 2385-2416.

Hafkenscheid, E., Wortel, M. J. R., & Spakman, W. (2006). Subduction history of the Tethyan region derived from seismic tomography and tectonic reconstructions. *Journal of Geophysical Research, 111*(B8).

Handy, M. R., Schmid, S. M., Bousquet, R., Kissling, E., & Bernoulli, D. (2010). Reconciling plate-tectonic reconstructions of Alpine Tethys with the geological–geophysical record of spreading and subduction in the Alps. *Earth-Science Reviews*, *102*(3-4), 121-158.

Hetzel, R., Ring, U., Akal, C. & Troesch, M. (1995). Miocene NNE-directed extensional unroofing in the Menderes Massif, southwestern Turkey. *Journal of the Geological Society 152*: 639-654.

Hodges, K. V. (2000). Tectonics of the Himalaya and southern Tibet from two perspectives. *Geological Society of America Bulletin*, *112*, 324-350.

Hu, X., Garzanti, E., Moore, T., and Raffi, I. (2015). Direct stratigraphic dating of India-Asia collision onset at the Selandian (middle Paleocene, 59 ± 1 Ma). *Geology*, *43*, 859-862.

Humphreys, E. (2009). Relation of flat subduction to magmatism and deformation in the western United States.

Keay, S., Lister, G. & Buick, I (2001). The timing of partial melting, Barrovian metamorphism and granite intrusion in the Naxos metamorphic core complex, Cyclades, Aegean Sea, Greece. *Tectonophysics 342*, 275-312.

IGRS-IFP. (1966). Étude Géologique de l'Epire (Grèce Nord-occidentale). In: Technip Paris.

Ilbeyli, N. (2005). Mineralogical–geochemical constraints on intrusives in central Anatolia, Turkey: tectono-magmatic evolution and characteristics of mantle source. *Geological Magazine, 142*(2), 187-207.

Ilbeyli, N., & Kibici, Y. (2009). Collision-related granite magma genesis, potential sources and tectono-magmatic evolution: comparison between central, northwestern and western Anatolia (Turkey). *International Geology Review, 51*(3), 252-278.

Isik, V. (2009). The ductile shear zone in granitoid of the Central Anatolian Crystalline Complex, Turkey: Implications for the origins of the Tuzgölü basin during the Late Cretaceous extensional deformation. *Journal of Asian Earth Sciences, 34*, 507-521.

Isik, V., Lo, C.-H., Göncüoğlu, C., & Demirel, S. (2008). 39Ar/40Ar Ages from the Yozgat Batholith: Preliminary Data on the Timing of Late Cretaceous Extension in the Central Anatolian Crystalline Complex, Turkey. *The Journal of Geology, 116*(5), 510-526.

Isik, V., Tekeli, O., & Seyitoglu, G. (2004). The 40Ar/39Ar age of extensional ductile deformation and granitoid intrusion in the northern Menderes core complex: implications for the initiation of extensional tectonics in western Turkey. *Journal of Asian Earth Sciences, 23*(4), 555-566.

Jackson, M., & Macdonald, F. (2022). Hemispheric geochemical dichotomy of the mantle is a legacy of austral supercontinent assembly and onset of deep continental crust subduction. *AGU Advances, 3*(6), e2022AV000664.

Jadoul, F., Berra, F. & Garzanti, E. (1998). The Tethys Himalayan passive margin from Late Triassic to Early Cretaceous (South Tibet). *Journal of Asian Earth Sciences, 16*, 173-194.

Jamieson, R. A., Beaumont, C., Fullsack, P., & Lee, B. (1998). Barrovian regional metamorphism: where's the heat? *Geological Society, London, Special Publications, 138*(1), 23-51.

Jamtveit, B., & Austrheim, H. (2010). Metamorphism: the role of fluids. *Elements, 6*(3), 153-158.

Jolivet, L., & Brun, J.-P. (2010). Cenozoic geodynamic evolution of the Aegean. *International Journal of Earth Sciences, 99*(1), 109-138.

Jolivet, L., Faccenna, C., Goffé, B., Burov, E., & Agard, P. (2003). Subduction tectonics and exhumation of high-pressure metamorphic rocks in the Mediterranean orogens. *American Journal of Science*, *303*(5), 353-409.

Jolivet, L., Goffé, B., Monié, P., Truffert-Luxey, C., Patriat, M., & Bonneau, M. (1996). Miocene detachment in Crete and exhumation P-T-t paths of high-pressure metamorphic rocks. *Tectonics, 15*(6), 1129-1153.

Jolivet, L., Lecomte, E., Huet, B., Denèle, Y., Lacombe, O., Labrousse, L., et al. (2010). The North Cycladic Detachment System. *Earth and Planetary Science Letters, 289*(1-2), 87-104.

Jolivet, L., Menant, A., Sternai, P., Rabillard, A., Arbaret, L., Augier, R., et al. (2015). The geological signature of a slab tear below the Aegean. *Tectonophysics, 659*, 166-182.

Jolivet, L., Trotet, F., Monié, P., Vidal, O., Goffé, B., Labrousse, L., et al. (2010). Along-strike variations of P–T conditions in accretionary wedges and syn-orogenic extension, the HP–LT Phyllite–Quartzite Nappe in Crete and the Peloponnese. *Tectonophysics, 480*(1-4), 133-148.

Kadıoğlu, Y. K., Dilek, Y., Güleç, N. & Foland, K.A. (2003). Tectonomagmatic evolution of bimodal plutons in the Central Anatolian Crystalline Complex, Turkey. *The Journal of Geology 111*, 671-690.

Kapp, P., & DeCelles, P. G. (2019). Mesozoic–Cenozoic geological evolution of the Himalayan-Tibetan orogen and working tectonic hypotheses. *American Journal of Science*, *319*(3), 159-254.

Karabulut, H., Paul, A., Afacan Ergün, T., Hatzfeld, D., Childs, D.M. & Aktar, M. (2013). Long-wavelength undulations of the seismic Moho beneath the strongly stretched Western Anatolia. *Geophysical Journal International 194,* 450-464.

Kastens, K. A. (1991). Rate of outward growth of the Mediterranean Ridge accretionary complex. *Tectonophysics*, *199*(1), 25-50.

Kay, S. M., & Mpodozis, C. (2002). Magmatism as a probe to the Neogene shallowing of the Nazca plate beneath the modern Chilean flat-slab. *Journal of South American Earth Sciences*, *15*(1), 39-57.

Kaymakci, N., Özçelik, Y., White, S. H., & Van Dijk, P. M. (2009). Tectono-stratigraphy of the Çankırı Basin: Late Cretaceous to early Miocene evolution of the Neotethyan Suture Zone in Turkey. *Geological Society, London, Special Publications*, *311*(1), 67-106.

Keay, S., & Lister, G. (2002). African provenance for the metasediments and metaigneous rocks of the Cyclades, Aegean Sea, Greece. *Geology*, *30*(3), 235-238.

Khanal, G. P., Wang, J. M., Larson, K. P., Wu, F. Y., Rai, S. M., Wang, J. G., & Yang, L. (2021). Eocene metamorphism and anatexis in the Kathmandu Klippe, Central Nepal: implications for early crustal thickening and initial rise of the Himalaya. *Tectonics, 40*(4), e2020TC006532.

Koç, A., Kaymakci, N., Van Hinsbergen, D. J. J., & Kuiper, K. F. (2017). Miocene tectonic history of the Central Tauride intramontane basins, and the paleogeographic evolution of the Central Anatolian Plateau. *Global and Planetary Change*, *158*, 83-102.

Köksal, S., Möller, A., Göncüoglu, M. C., Frei, D., & Gerdes, A. (2012). Crustal homogenization revealed by U–Pb zircon ages and Hf isotope evidence from the Late Cretaceous granitoids of the Agaçören intrusive suite (Central Anatolia/Turkey). *Contributions to Mineralogy and Petrology*, *163*, 725-743.

Köksal, S., Romer, R. L., Göncüoglu, M. C., & Toksoy-Köksal, F. (2004). Timing of post-collisional H-type to A-type granitic magmatism: U–Pb titanite ages from the Alpine central Anatolian granitoids (Turkey). *International Journal of Earth Sciences*, *93*(6), 974-989.

Kotowski, A. J., & Behr, W. M. (2019). Length scales and types of heterogeneities along the deep subduction interface: Insights from exhumed rocks on Syros Island, Greece. *Geosphere*, *15*(4), 1038-1065.

Kotowski, A. J., Cisneros, M., Behr, W. M., Stockli, D. F., Soukis, K., Barnes, J. D., & Ortega-Arroyo, D. (2022). Subduction, underplating, and return flow recorded in the Cycladic Blueschist Unit exposed on Syros, Greece. *Tectonics*, *41*(6), e2020TC006528.

Krahl, J., Kauffmann, G., Kozur, H., Richter, D., Förster, O., & Heinritzi, F. (1983). Neue Daten zur biostratigraphie und zur tektonischen lagerung der Phyllit-Gruppe und der Trypali-Gruppe auf der Insel Kreta (Griechenland). *Geologische Rundschau*, *72*(3), 1147-1166.

Lagos, M., Scherer, E. E., Tomaschek, F., Münker, C., Keiter, M., Berndt, J., & Ballhaus, C. (2007). High precision Lu–Hf geochronology of Eocene eclogite-facies rocks from Syros, Cyclades, Greece. *Chemical Geology, 243*(1-2), 16-35.

Lamont, T. N., Roberts, N. M., Searle, M. P., Gardiner, N. J., Gopon, P., Hsieh, Y.-T., et al. (2023a). Contemporaneous crust-derived I-and S-type granite magmatism and normal faulting on Tinos, Delos, and Naxos, Greece: Constraints on Aegean orogenic collapse. *Geological Society of America Bulletin*.

Lamont, T. N., Roberts, N. M., Searle, M. P., Gopon, P., Waters, D. J., & Millar, I. (2020a). The age, origin, and emplacement of the Tsiknias Ophiolite, Tinos, Greece. *Tectonics, 39*(1), e2019TC005677.

Lamont, T. N., Searle, M. P., Gopon, P., Roberts, N. M., Wade, J., Palin, R. M., & Waters, D. J. (2020b). The Cycladic Blueschist Unit on Tinos, Greece: Cold NE subduction and SW directed extrusion of the Cycladic continental margin under the Tsiknias Ophiolite. *Tectonics, 39*(9), e2019TC005890.

Lamont, T. N., Searle, M.P., Waters, D.J., Roberts, N.M.W., Palin, R.M., Smye, A., Dyck, B., Gopon, P., Weller, O.M., St-Onge, M.R (2020c). Compressional origin of the Naxos metamorphic core complex, Greece: Structure, petrography, and thermobarometry. *Geological Society of America Bulletin 132*: 149-197.

Lamont, T. N., Smye, A. J., Roberts, N. M., Searle, M. P., Waters, D. J., & White, R. W. (2023b). Constraints on the thermal evolution of metamorphic core complexes from the timing of high-pressure metamorphism on Naxos, Greece. *Geological Society of America Bulletin 135*, 2676-2796.

Laurent, V., Huet, B., Labrousse, L., Jolivet, L., Monie, P., & Augier, R. (2017). Extraneous argon in high-pressure metamorphic rocks: Distribution, origin and transport in the Cycladic Blueschist Unit (Greece). *Lithos, 272,* 315-335.

Leech, M., Singh, S., Jain, A., Klemperer, S., & Manickavasagam, R. (2005). The onset of India–Asia continental collision: Early, steep subduction required by the timing of UHP metamorphism in the western Himalaya. *Earth and Planetary Science Letters, 234*(1-2), 83-97.

Lefebvre, C. (2011). *The tectonics of the Central Anatolian Crystalline Complex: a structural, metamorphic and paleomagnetic study (PhD thesis)* (Vol. 3).

Lefebvre, C., Barnhoorn, A., van Hinsbergen, D. J. J., Kaymakci, N., & Vissers, R. L. M. (2011). Late Cretaceous extensional denudation along a marble detachment fault zone in the Kırşehir massif near Kaman, central Turkey. *Journal of Structural Geology, 33*(8), 1220-1236.

Lefebvre, C., Meijers, M. J. M., Kaymakci, N., Peynircioğlu, A., Langereis, C. G., & van Hinsbergen, D. J. J. (2013). Reconstructing the geometry of central Anatolia during the late Cretaceous: Large-scale Cenozoic rotations and deformation between the Pontides and Taurides. *Earth and Planetary Science Letters, 366*, 83-98.

Lefebvre, C., Peters, M. K., Wehrens, P. C., Brouwer, F. M., & van Roermund, H. L. M. (2015). Thermal history and extensional exhumation of a high-temperature crystalline complex (Hırkadağ Massif, Central Anatolia). *Lithos, 238*, 156-173. http://www.sciencedirect.com/science/article/pii/S0024493715003424

Lips, A. L. W., Cassard, D., Sözbilir, H., Yilmaz, H., & Wijbrans, J. R. (2001). Multistage exhumation of the Menderes Massif, western Anatolia (Turkey). *International Journal of Earth Sciences, 89*(4), 781-792.

Lister, G. S., Banga, G. & Feenstra, A. (1984). Metamorphic core complexes of Cordilleran type in the Cyclades, Aegean Sea, Greece. *Geology 12,* 221-225

Liu, L., Shi, D., Klemperer, S. L., & Shi, J. (2023). Slab tearing and delamination of the Indian lithospheric mantle during flat-slab subduction, southeast Tibet. *Authorea Preprints*.

Maffione, M., van Hinsbergen, D. J. J., de Gelder, G. I. N. O., van der Goes, F. C., & Morris, A. (2017). Kinematics of Late Cretaceous subduction initiation in the Neo-Tethys Ocean reconstructed from ophiolites of Turkey, Cyprus, and Syria. *Journal of Geophysical Research: Solid Earth*, *122*(5), 3953-3976.

Marsellos, A. E., Kidd, W. S. F., & Garver, J. I. (2010). Extension and exhumation of the HP/LT rocks in the Hellenic forearc ridge. *American Journal of Science, 310,* 1-36.

Martin, L., Duchêne, S., Deloule, E., and Vanderhaeghe, O. (2006). The isotopic composition of zircon and garnet: A record of the metamorphic history of Naxos, Greece. *Lithos 87,* 174-192.

McPhee, P. J., Altıner, D., & van Hinsbergen, D. J. J. (2018). First Balanced Cross Section Across the Taurides Fold-Thrust Belt: Geological Constraints on the Subduction History of the Antalya Slab in Southern Anatolia. *Tectonics*.

McPhee, P. J., Koç, A., & van Hinsbergen, D. J. J. (2022). Preparing the ground for plateau growth: Late Neogene Central Anatolian uplift in the context of orogenic and geodynamic evolution since the Cretaceous. *Tectonophysics, 822*, 229131.

McPhee, P. J., van Hinsbergen, D. J. J., & Thomson, S. (2019). Thermal history of the western Central Taurides fold-thrust belt: Implications for Cenozoic vertical motions of southern Central Anatolia. *Geosphere, 15,* 1927-1942.

Memiş, C., Göğüş, O. H., Uluocak, E. Ş., Pysklywec, R., Keskin, M., Şengör, A. C., & Topuz, G. (2020). Long wavelength progressive plateau uplift in Eastern Anatolia since 20 Ma: implications for the role of slab peel-Back and Break-off. *Geochemistry, Geophysics, Geosystems, 21*(2), e2019GC008726.

Molnar, N. E., Cruden, A.R. & Betts, P.G. (2018). Unzipping continents and the birth of microcontinents. *Geology 46,* 451-454.

Mueller, M., Licht, A., Campbell, C., Ocakoğlu, F., Taylor, M., Burch, L., et al. (2019). Collision chronology along the İzmir-Ankara-Erzincan suture zone: Insights from the Sarıcakaya Basin, western Anatolia. *Tectonics, 38*(10), 3652-3674.

Mulcahy, S. R., Vervoort, J. D., & Renne, P. R. (2014). Dating subduction-zone metamorphism with combined garnet and lawsonite Lu–Hf geochronology. *Journal of Metamorphic Geology, 32*(5), 515-533. https://doi.org/10.1111/jmg.12092

Ocakoğlu, F., Hakyemez, A., Açıkalın, S., Özkan Altıner, S., Büyükmeriç, Y., Licht, A., et al. (2019). Chronology of subduction and collision along the İzmir-Ankara suture in Western Anatolia: records from the Central Sakarya Basin. *International Geology Review, 61*(10), 1244-1269.

Okay, A. (2002). Jadeite–chloritoid–glaucophane–lawsonite blueschists in north-west Turkey: unusually high P/T ratios in continental crust. *Journal of Metamorphic Geology, 20*(8), 757-768.

Okay, A. I. (2001). Stratigraphic and metamorphic inversions in the central Menderes Massif: a new structural model. *International Journal of Earth Sciences, 89*(4), 709-727.

Okay, A. I., Satir, M., Maluski, H., Siyako, M., Monie, P., Metzger, R., & Akyüz, S. (1996). Paleo-and Neo-Tethyan events in northwestern Turkey: geologic and geochronologic constraints. *World and Regional Geology*, 420-441.

Okay, A. I., & Whitney, D. L. (2010). Blueschists, eclogites, ophiolites and suture zones in northwest Turkey: a review and a field excursion guide. *Ofioliti, 35*(2), 131-172.

Önen, A. P. (2003). Neotethyan ophiolitic rocks of the Anatolides of NW Turkey and comparison with Tauride ophiolites. *Journal of the Geological Society, 160,* 947-962.

Önen, A. P., & Hall, R. (1993). Ophiolites and related metamorphic rocks from the Kütahya region, north-west Turkey. *Geological Journal, 160*, 947-962.

Özer, S., & Sözbilir, H. (2003). Presence and tectonic significance of Cretaceous rudist species in the so-called Permo-Carboniferous Göktepe Formation, central Menderes metamorphic massif, western Turkey. *International Journal of Earth Sciences, 92*(3), 397-404. https://doi.org/10.1007/s00531-003-0333-z

Ozgenc, I., & Ilbeyli, N. (2008). Petrogenesis of the Late Cenozoic Egrigöz pluton in western Anatolia, Turkey: implications for magma genesis and crustal processes. *International Geology Review, 50*(4), 375-391.

Özgül, N. (1976). Some geological aspects of the Taurus orogenic belt (Turkey). *Bulletin of the Geological Society of Turkey 19*, 65-78.

Palin, R. M., Reuber, G. S., White, R. W., Kaus, B. J., & Weller, O. M. (2017). Subduction metamorphism in the Himalayan ultrahigh-pressure Tso Morari massif: an integrated geodynamic and petrological modelling approach. *Earth and Planetary Science Letters, 467*, 108-119.

Parlak, O. (2016). The tauride ophiolites of Anatolia (Turkey): A review. *Journal of Earth Science, 27*(6), 901-934.

Pastor-Galán, D., Mulchrone, K.F., Koymans, M.R., van Hinsbergen, D.J.J. & Langereis, C.G. (2017). Bootstrapped total least squares orocline test: A robust method to quantify vertical-axis rotation patterns in orogens, with examples from the Cantabrian and Aegean oroclines. *Lithosphere, 9*, 499-511.

Peillod, A., Ring, U., Glodny, J., & Skelton, A. (2017). An Eocene/Oligocene blueschist-/greenschist facies P–T loop from the Cycladic Blueschist Unit on Naxos Island, Greece: Deformation-related re-equilibration vs. thermal relaxation. *Journal of Metamorphic Geology, 35*(7), 805-830.

Pe-Piper, G. (2000). Origin of S-type granites coeval with I-type granites in the Hellenic subduction system, Miocene of Naxos, Greece. *European Journal of Mineralogy 12*, 859-875.

Pe-Piper, G., et al. (2002). The igneous rocks of Greece: the anatomy of an orogen, Gebrüder Borntraeger. Berlin–Stuttgart, Germany.

Philippon, M., Brun, J.-P., and Gueydan, F. (2012). Deciphering subduction from exhumation in the segmented Cycladic Blueschist Unit (Central Aegean, Greece). *Tectonophysics 524-525*, 116-134.

Platt, J. (1986). Dynamics of orogenic wedges and the uplift of high-pressure metamorphic rocks. *Geological Society of America Bulletin, 97*(9), 1037-1053.

Platt, J. P., & Vissers, R. L. M. (1989). Extensional collapse of thickened continental lithosphere: A working hypothesis for the Alboran Sea and Gibraltar arc. *Geology, 17*(6), 540-543.

Plunder, A., Agard, P., Chopin, C., & Okay, A. I. (2013). Geodynamics of the Tavşanlı zone, western Turkey: Insights into subduction/obduction processes. *Tectonophysics, 608,* 884-903.

Plunder, A., Agard, P., Chopin, C., Soret, M., Okay, A.I., & Whitechurch, H. (2016). Metamorphic sole formation, emplacement and blueschist facies overprint: early subduction dynamics witnessed by western Turkey ophiolites. *Terra Nova, 28,* 329-339.

Plunder, A., Thieulot, C., & van Hinsbergen, D. J. J. (2018). The effect of obliquity on temperature in subduction zones: insights from 3-D numerical modeling. *Solid Earth, 9*(3), 759-776.

Pourteau, A., Candan, O., & Oberhänsli, R. (2010). High-pressure metasediments in central Turkey: Constraints on the Neotethyan closure history. *Tectonics, 29*(5), n/a-n/a.

Pourteau, A., Scherer, E. E., Schorn, S., Bast, R., Schmidt, A., & Ebert, L. (2019). Thermal evolution of an ancient subduction interface revealed by Lu–Hf garnet geochronology, Halilbağı Complex (Anatolia). *Geoscience Frontiers, 10,* 127-148.

Pourteau, A., Oberhänsli, R., Candan, O., Barrier, E. & Vrielynck, B. (2016). Neotethyan closure history of western Anatolia: a geodynamic discussion. *International Journal of Earth Sciences, 105,* 203-224.

Pourteau, A., Sudo, M., Candan, O., Lanari, P., Vidal, O., & Oberhänsli, R. (2013). Neotethys closure history of Anatolia: insights from 40Ar-39Ar geochronology andP-Testimation in high-pressure metasedimentary rocks. *Journal of Metamorphic Geology, 31*(6), 585-606.

Rahl, J., Anderson, K., Brandon, M., & Fassoulas, C. (2005). Raman spectroscopic carbonaceous material thermometry of low-grade metamorphic rocks: Calibration and application to tectonic exhumation in Crete, Greece. *Earth and Planetary Science Letters, 240*(2), 339-354.

Régnier, J., Ring, U., Passchier, C.W., Gessner, K. & Güngör, T. (2003). Contrasting metamorphic evolution of metasedimentary rocks from the Cine and Selimiye nappes in the Anatolide belt, western Turkey. *Journal of Metamorphic Geology, 21*, 699-721.

Rimmelé, G., Oberhänsli, R., Goffé, B., Jolivet, L., Candan, O., & Çetinkaplan, M. (2003). First evidence of high-pressure metamorphism in the “Cover Series” of the southern Menderes Massif. Tectonic and metamorphic implications for the evolution of SW Turkey. *Lithos, 71*(1), 19-46.

Ring, U., Gessner, K., Güngör, T. & Passchier, C.W. (1999). The Menderes Massif of western Turkey and the Cycladic Massif in the Aegean—do they really correlate? *Journal of the Geological Society 156*: 3-6.

Ring, U., & Collins, A. S. (2005). U-Pb SIMS dating of synkinematic granites: timing of core-complex formation in the northern Anatolide belt of western Turkey. *Journal of the Geological Society, 162*(2), 289-298.

Ring, U., Glodny, J., Will, T., & Thomson, S. (2007a). An Oligocene extrusion wedge of blueschist-facies nappes on Evia, Aegean Sea, Greece: implications for the early exhumation of high-pressure rocks. *Journal of the Geological Society, 164*(3), 637-652.

Ring, U., & Layer, P. W. (2003). High-pressure metamorphism in the Aegean, eastern Mediterranean: Underplating and exhumation from the Late Cretaceous until the Miocene to Recent above the retreating Hellenic subduction zone. *Tectonics, 22*(3)

Ring, U., Layer, P. W., & Reischmann, T. (2001). Miocene high-pressure metamorphism in the Cyclades and Crete, Aegean Sea, Greece: Evidence for large-magnitude displacement on the Cretan detachment. *Geology, 29*(5), 395-398.

Ring, U., Will, T., Glodny, J., Kumerics, C., Gessner, K., Thomson, S., et al. (2007b). Early exhumation of high-pressure rocks in extrusion wedges: Cycladic blueschist unit in the eastern Aegean, Greece, and Turkey. *Tectonics, 26*(2), n/a-n/a.

Robertson, A. H. F. (2002). Overview of the genesis and emplacement of Mesozoic ophiolites in the Eastern Mediterranean Tethyan region. *Lithos 65*: 1-67.

Roche, V., Jolivet, L., Papanikolaou, D., Bozkurt, E., Menant, A., and Rimmelé, G. (2019). Slab fragmentation beneath the Aegean/Anatolia transition zone: Insights from the tectonic and metamorphic evolution of the Eastern Aegean region. *Tectonophysics 754*: 101-129.

Romano, S. S., Dörr, W., & Zulauf, G. (2004). Cambrian granitoids in pre-Alpine basement of Crete (Greece): evidence from U-Pb dating of zircon. *International Journal of Earth Sciences, 93*(5), 844-859.

Schmid, S. M., Bernoulli, D., Fügenschuh, B., Georgiev, N., Kounov, A., Matenco, L., et al. (2020). Tectonic units of the Alpine collision zone between Eastern Alps and Western Turkey. *Gondwana Research, 78,* 308-374.

Schmid, S.M., Scharf, A., Handy, M.R. and Rosenberg, C.L (2013). The Tauern Window (Eastern Alps, Austria): a new tectonic map, with cross-sections and a tectonometamorphic synthesis. *Swiss Journal of Geosciences, 106(1),* 1-32.

Schmidt, A., Pourteau, A., Candan, O., & Oberhänsli, R. (2015). Lu–Hf geochronology on cm-sized garnets using microsampling: New constraints on garnet growth rates and duration of metamorphism during continental collision (Menderes Massif, Turkey). *Earth and Planetary Science Letters, 432*, 24-35.

Searle, M. P., & Lamont, T. N. (2020). Compressional metamorphic core complexes, low-angle normal faults and extensional fabrics in compressional tectonic settings. *Geological Magazine, 157*(1), 101-118.

Seaton, N. C. A., Teyssier, C., Whitney, D. L., & Heizler, M. T. (2014). Quartz and calcite microfabric transitions in a pressure and temperature gradient, Sivrihisar, Turkey. *Geodinamica Acta, 26*(3-4), 191-206.

Seidel, E. (1978). Zur petrologiedes Phyllit-Quartzit Serie Kreta, *PhD Thesis, Braunschweig University, Germany*.

Şengör, A. M. C., & Yilmaz, Y. (1981). Tethyan evolution of Turkey: A plate tectonic approach. *Tectonophysics, 75*(3), 181-241.

Seyitoğlu, G., Isik, V., Gürbüz, E., & Gürbüz, A. (2017). The discovery of a low-angle normal fault in the Taurus Mountains: the İvriz detachment and implications concerning the Cenozoic geology of southern Turkey. *Turkish Journal of Earth Sciences, 26*, 189-205.

Shaked, Y., Avigad, D. & Garfunkel, Z. (2000). Alpine high-pressure metamorphism at the Almyropotamos window (southern Evia, Greece). *Geological Magazine 137,* 367-380.

Skelton, A., Peillod, A., Glodny, J., Klonowska, I., Månbro, C., Lodin, K., & Ring, U. (2019). Preservation of high-P rocks coupled to rock composition and the absence of metamorphic fluids. *Journal of Metamorphic Geology, 37*(3), 359-381.

Smit, M. A., Hacker, B. R., & Lee, J. (2014). Tibetan garnet records early Eocene initiation of thickening in the Himalaya. *Geology, 42*(7), 591-594.

Smye, A. J., Bickle, M. J., Holland, T. J., Parrish, R. R., & Condon, D. J. (2011). Rapid formation and exhumation of the youngest Alpine eclogites: a thermal conundrum to Barrovian metamorphism. *Earth and Planetary Science Letters, 306*(3-4), 193-204.

Soder, C., Altherr, R., & Romer, R. L. (2016). Mantle metasomatism at the edge of a retreating subduction zone: Late Neogene lamprophyres from the Island of Kos, Greece. *Journal of Petrology, 57*(9), 1705-1728.

Sotiropoulos, S., Kamberis, E., Triantaphyllou, M. V., & Doutsos, T. (2003). Thrust sequences in the central part of the External Hellenides. *Geological Magazine, 140*(6), 661-668.

Spakman, W., & Hall, R. (2010). Surface deformation and slab–mantle interaction during Banda arc subduction rollback. *Nature Geoscience, 3*, 562-566.

Stampfli, G. M. & C. Hochard (2009). Plate tectonics of the Alpine realm. *Geological Society, London, Special Publications, 327*, 89-111.

Stern, R. J. (2002). Subduction zones. *Reviews of Geophysics, 40*, doi: 10.1029/2001rg000108

St-Onge, M. R., Searle, M. P., & Wodicka, N. (2006). Trans‐Hudson Orogen of North America and Himalaya‐Karakoram‐Tibetan Orogen of Asia: Structural and thermal characteristics of the lower and upper plates. *Tectonics, 25*(4).

Stübner, K., Grujic, D., Parrish, R. R., Roberts, N. M. W., Kronz, A., Wooden, J., & Ahmad, T. (2014). Monazite geochronology unravels the timing of crustal thickening in NW Himalaya. *Lithos, 210-211*, 111-128.

Tezel, T., Shibutani, T., & Kaypak, B. (2013). Crustal thickness of Turkey determined by receiver function. *Journal of Asian Earth Sciences, 75*, 36-45.

Theye, T., Seidel, E., & Vidal, O. (1992). Carpholite, sudoite, and chloritoid in low-grade high-pressure metapelites from Crete and the Peloponnese, Greece. *European Journal of Mineralogy, 4*(3), 487-507.

Thomson, S. N., Stöckhert, B. & Brix, M.R. (1998). Thermochronology of the high-pressure metamorphic rocks of Crete, Greece: Implications for the speed of tectonic processes. *Geology 26*, 259-263.

Thomson, S. N., Stöckhert, B., & Brix, M. R. (1999). Miocene high-pressure metamorphic rocks of Crete, Greece: rapid exhumation by buoyant escape. *Geological Society, London, Special Publications, 154*, 87-107.

Tirel, C., Brun, J. P., Burov, E., Wortel, M. J. R., & Lebedev, S. (2013). A plate tectonics oddity: Caterpillar-walk exhumation of subducted continental crust. *Geology, 41*(5), 555-558.

Tirel, C., Gueydan, F., Tiberi, C., & Brun, J.-P. (2004). Aegean crustal thickness inferred from gravity inversion. Geodynamical implications. *Earth and Planetary Science Letters, 228*, 267-280.

Tomaschek, F. (2003). Zircons from Syros, Cyclades, Greece--Recrystallization and Mobilization of Zircon During High-Pressure Metamorphism. *Journal of Petrology, 44*, 1977-2002.

Toussaint, G., Burov, E., & Avouac, J. P. (2004). Tectonic evolution of a continental collision zone: A thermomechanical numerical model. *Tectonics, 23*.

Tual, L., Smit, M. A., Cutts, J., Kooijman, E., Kielman-Schmitt, M., Majka, J., & Foulds, I. (2022). Rapid, paced metamorphism of blueschists (Syros, Greece) from laser-based zoned Lu-Hf garnet chronology and LA-ICPMS trace element mapping. *Chemical Geology, 607*, 121003.

Underhill, J. R. (1989). Late Cenozoic deformation of the Hellenide foreland, western Greece. Geological Society of America Bulletin, *101*, 613-634.

Uunk, B., Brouwer, F., de Paz-Álvarez, M., van Zuilen, K., Huybens, R., van't Veer, R., & Wijbrans, J. (2022). Consistent detachment of supracrustal rocks from a fixed subduction depth in the Cyclades. *Earth and Planetary Science Letters, 584*, 117479.

Vanderhaeghe, O., Kruckenberg, S.C., Gerbault, M., Martin, L., Duchêne, S., Deloule, E. (2018). Crustal-scale convection and diapiric upwelling of a partially molten orogenic root (Naxos dome, Greece). *Tectonophysics 746*, 459-469.

van de Lagemaat, S. H., Swart, M. L., Vaes, B., Kosters, M. E., Boschman, L. M., Burton-Johnson, A., et al. (2021). Subduction initiation in the Scotia Sea region and opening of the Drake Passage: When and why? *Earth-Science Reviews*, 103551.

van Hinsbergen, D. J. J., Gürer, D., Koç, A., and Lom, N. (2024). Shortening and extrusion in the East Anatolian Plateau: How was Neogene Arabia-Eurasia convergence tectonically accommodated? *Earth and Planetary Science Letters*, *641*, 118827.

van Hinsbergen, D. J. J., Hafkenscheid, E., Spakman, W., Meulenkamp, J. E., & Wortel, R. (2005a). Nappe stacking resulting from subduction of oceanic and continental lithosphere below Greece. *Geology, 33*(4).

van Hinsbergen, D. J. J., Kaymakci, N., Spakman, W., & Torsvik, T. H. (2010). Reconciling the geological history of western Turkey with plate circuits and mantle tomography. *Earth and Planetary Science Letters, 297*(3-4), 674-686.

van Hinsbergen, D. J. J., Lippert, P. C., Li, S., Huang, W., Advokaat, E. L., & Spakman, W. (2019). Reconstructing Greater India: Paleogeographic, kinematic, and geodynamic perspectives. *Tectonophysics, 760*, 69-94.

van Hinsbergen, D. J. J., Maffione, M., Plunder, A., Kaymakci, N., Ganerød, M., Hendriks, B. W. H., et al. (2016). Tectonic evolution and paleogeography of the Kırşehir Block and the Central Anatolian Ophiolites, Turkey. *Tectonics, 35*, 983-1014.

van Hinsbergen, D. J. J., Peters, K., Maffione, M., Spakman, W., Guilmette, C., Thieulot, C., Plümper, O., Gürer, D., Brouwer, F.M., Aldanmaz, E., Kaymakci, N. (2015). Dynamics of intraoceanic subduction initiation: 2. Suprasubduction zone ophiolite formation and metamorphic sole exhumation in context of absolute plate motions. *Geochemistry, Geophysics, Geosystems*, *16*, 1771-1785.

van Hinsbergen, D. J. J., & Schmid, S. M. (2012). Map view restoration of Aegean-West Anatolian accretion and extension since the Eocene. *Tectonics, 31*(5), n/a-n/a.

van Hinsbergen, D. J. J., & Schouten, T. L. A. (2021). Deciphering paleogeography from orogenic architecture: constructing orogens in a future supercontinent as thought experiment. *American Journal of Science, 321*, 955-1031.

van Hinsbergen, D. J. J., Torsvik, T., Schmid, S. M., Matenco, L., Maffione, M., Vissers, R. L. M., et al. (2020). Orogenic architecture of the Mediterranean region and kinematic reconstruction of its tectonic evolution since the Triassic. *Gondwana Research, 81*, 79-229.

van Hinsbergen, D. J. J., van der Meer, D. G., Zachariasse, W. J., & Meulenkamp, J. E. (2006). Deformation of western Greece during Neogene clockwise rotation and collision with Apulia. *International Journal of Earth Sciences, 95*(3), 463-490.

van Hinsbergen, D. J. J., Zachariasse, W. J., Wortel, M. J. R., & Meulenkamp, J. E. (2005b). Underthrusting and exhumation: A comparison between the External Hellenides and the "hot" Cycladic and "cold" South Aegean core complexes (Greece). *Tectonics, 24*(2), n/a-n/a.

Wardle, R. J., James, D. T., Scott, D. J., & Hall, J. (2002). The southeastern Churchill Province: synthesis of a Paleoproterozoic transpressional orogen. *Canadian Journal of Earth Sciences, 39*(5), 639-663.

Weller, O. M., St-Onge, M. R., Waters, D. J., Rayner, N., Searle, M. P., Chung, S. L., et al. (2013). Quantifying Barrovian metamorphism in the Danba Structural Culmination of eastern Tibet. *Journal of Metamorphic Geology, 31*(9), 909-935.

Whitney, D. L., & Bozkurt, E. (2002). Metamorphic history of the southern Menderes massif, western Turkey. *GSA Bulletin, 114*(7), 829-838.

Whitney, D. L., & Dilek, Y. (1998). Metamorphism during Alpine Crustal Thickening and Extension in Central Anatolia, Turkey: the Niğde Metamorphic Core Complex. *Journal of Petrology, 39*(7), 1385-1403.

Whitney, D. L., & Hamilton, M. A. (2004). Timing of high-grade metamorphism in central Turkey and the assembly of Anatolia. *Journal of the Geological Society, 161*(5), 823-828.

Whitney, D. L., Teyssier, C., Fayon, A. K., Hamilton, M. A., & Heizler, M. (2003). Tectonic controls on metamorphism, partial melting, and intrusion: timing and duration of regional metamorphism and magmatism in the Niğde Massif, Turkey. *Tectonophysics, 376*(1-2), 37-60.

Wolfe, O. M., Spear, F. S., Thomas, J. B., Hasegawa, E. M., Libby, G. T., & Cheney, J. T. (2023). Pressure–temperature evolution of the basement and cover sequences on Ios, Greece: Evidence for subduction of the Hercynian basement. *Journal of Metamorphic Geology, 41*(8), 1119-1141.

Yaliniz, M., P. A. Floyd & M. C. Göncüoğlu (1996), Supra-subduction zone ophiolites of Central Anatolia: Geochemical evidence from the Sarikaraman ophiolite, Aksaray, Turkey, Mineral. Mag., 60, 697–710.

Yalınız, M. K. (2008), A geochemical attempt to distinguish forearc and back arc ophiolites from the"supra-subuduction" Central Anatolian ophiolites (Turkey) by comparison with modern oceanic analogues, Ofoliti, 33, 119–129.

Zachariasse, W. J., van Hinsbergen, D. J. J., & Fortuin, A. R. (2011). Formation and fragmentation of a late Miocene supradetachment basin in central Crete: implications for exhumation mechanisms of high-pressure rocks in the Aegean forearc. *Basin Research, 23*(6), 678-701.

Zimmerman, A., Stein, H,J., Hannah, J.L., Koželj, D., Bogdanov, K., & Berza, T. (2007). Tectonic configuration of the Apuseni–Banat—Timok–Srednogorie belt, Balkans-South

Carpathians, constrained by high precision Re–Os molybdenite ages. *Mineralium Deposita*, *43*, 1-21.

**Figure 1.**

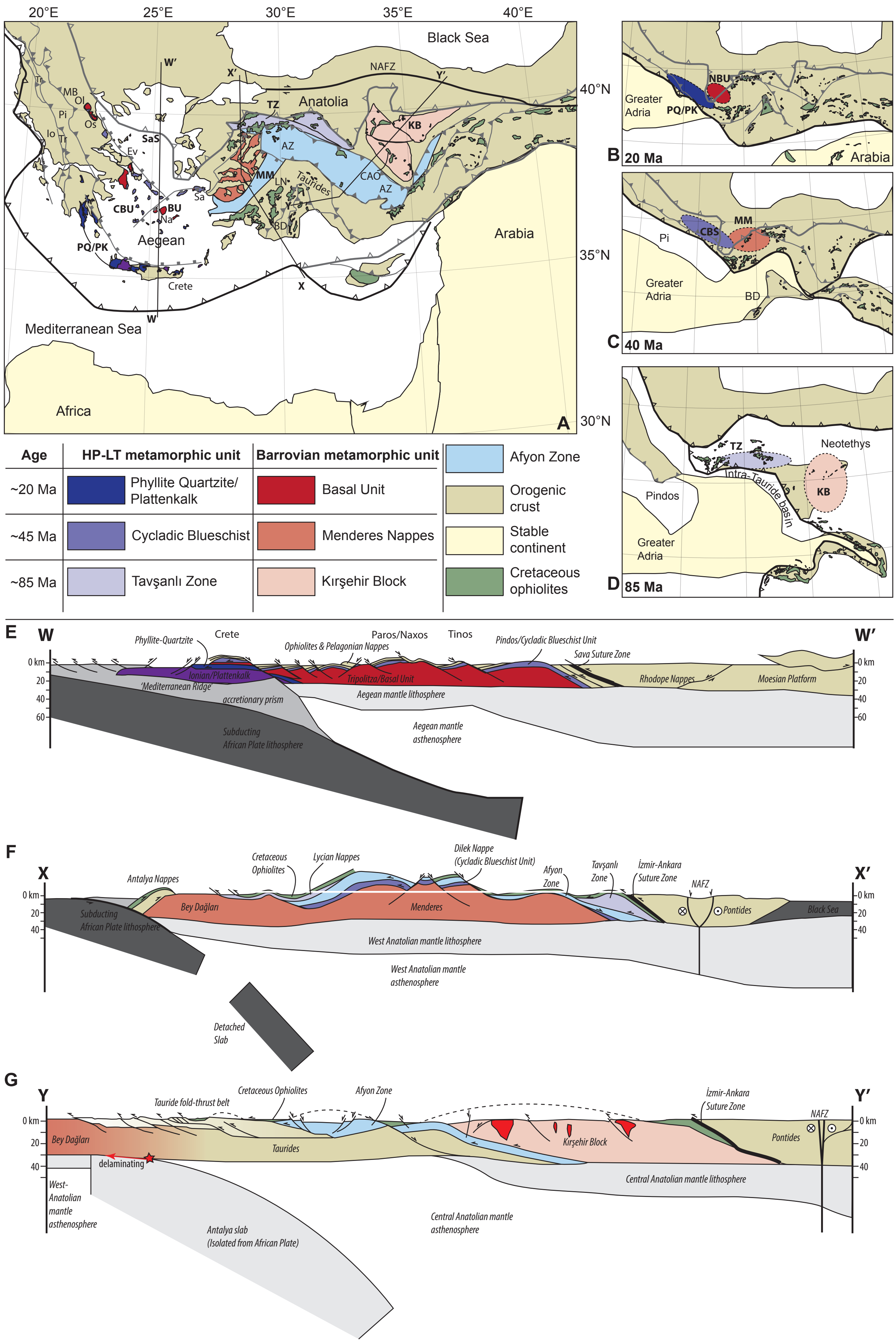

20°E
25°E
30°E
35°E
40°E
40°N
35°N
30°N
Black Sea
NAFZ
Anatolia
TZ
KB
AZ
MM
LN
Taurides
CAO
BD
SaS
Ev
Sa
CBU
BU
Na
Aegean
PQ/PK
Crete
MB
Ol
Os
Pi
Io
Tr
Arabia
Mediterranean Sea
Africa
W
W'
X
X'
Y
Y'
A
Greater Adria
NBU
B
20 Ma
CBS
MM
Pi
Greater Adria
BD
C
40 Ma
TZ
Neotethys
Intra-Tauride basin
Pindos
KB
Greater Adria
D
85 Ma
Age
HP-LT metamorphic unit
Barrovian metamorphic unit
~20 Ma
Phyllite Quartzite/ Plattenkalk
Basal Unit
~45 Ma
Cycladic Blueschist
Menderes Nappes
~85 Ma
Tavşanlı Zone
Kırşehir Block
Afyon Zone
Orogenic crust
Stable continent
Cretaceous ophiolites
E
Phyllite-Quartzite
Crete
Ophiolites & Pelagonian Nappes
Paros/Naxos
Tinos
Pindos/Cycladic Blueschist Unit
Sava Suture Zone
0 km
20
40
60
Ionian/Plattenkalk
'Mediterranean Ridge'
accretionary prism
Tripolitza/Basal Unit
Aegean mantle lithosphere
Rhodope Nappes
Moesian Platform
Subducting African Plate lithosphere
Aegean mantle asthenosphere
F
Antalya Nappes
Cretaceous Ophiolites
Lycian Nappes
Dilek Nappe (Cycladic Blueschist Unit)
Afyon Zone
Tavşanlı Zone
İzmir-Ankara Suture Zone
NAFZ
Bey Dağları
Menderes
Pontides
Black Sea
Subducting African Plate lithosphere
West Anatolian mantle lithosphere
West Anatolian mantle asthenosphere
Detached Slab
G
Tauride fold-thrust belt
Cretaceous Ophiolites
Afyon Zone
İzmir-Ankara Suture Zone
NAFZ
Bey Dağları
Taurides
Kırşehir Block
Pontides
delaminating
Central Anatolian mantle lithosphere
West-Anatolian mantle asthenosphere
Central Anatolian mantle asthenosphere
Antalya slab (Isolated from African Plate)

**Figure 2.**

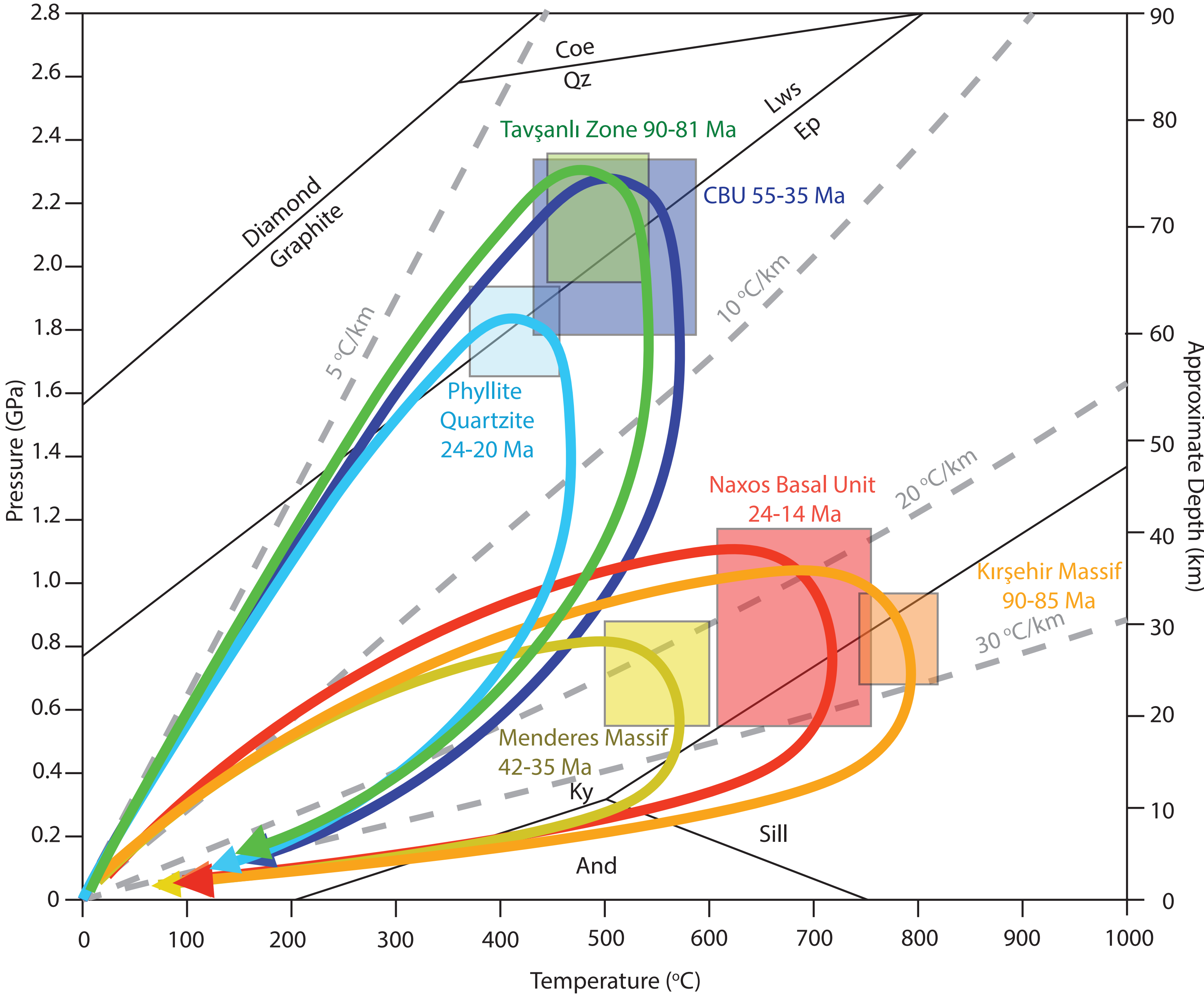

Pressure (GPa)
2.8
2.6
2.4
2.2
2.0
1.8
1.6
1.4
1.2
1.0
0.8
0.6
0.4
0.2
0
0
100
200
300
400
500
600
700
800
900
1000
Temperature (°C)
Approximate Depth (km)
90
80
70
60
50
40
30
20
10
0
Coe
Qz
Diamond
Graphite
Lws
Ep
5 °C/km
10 °C/km
20 °C/km
30 °C/km
Tavşanlı Zone 90-81 Ma
CBU 55-35 Ma
Phyllite
Quartzite
24-20 Ma
Naxos Basal Unit
24-14 Ma
Kırşehir Massif
90-85 Ma
Menderes Massif
42-35 Ma
Ky
Sill
And

**Figure 3.**

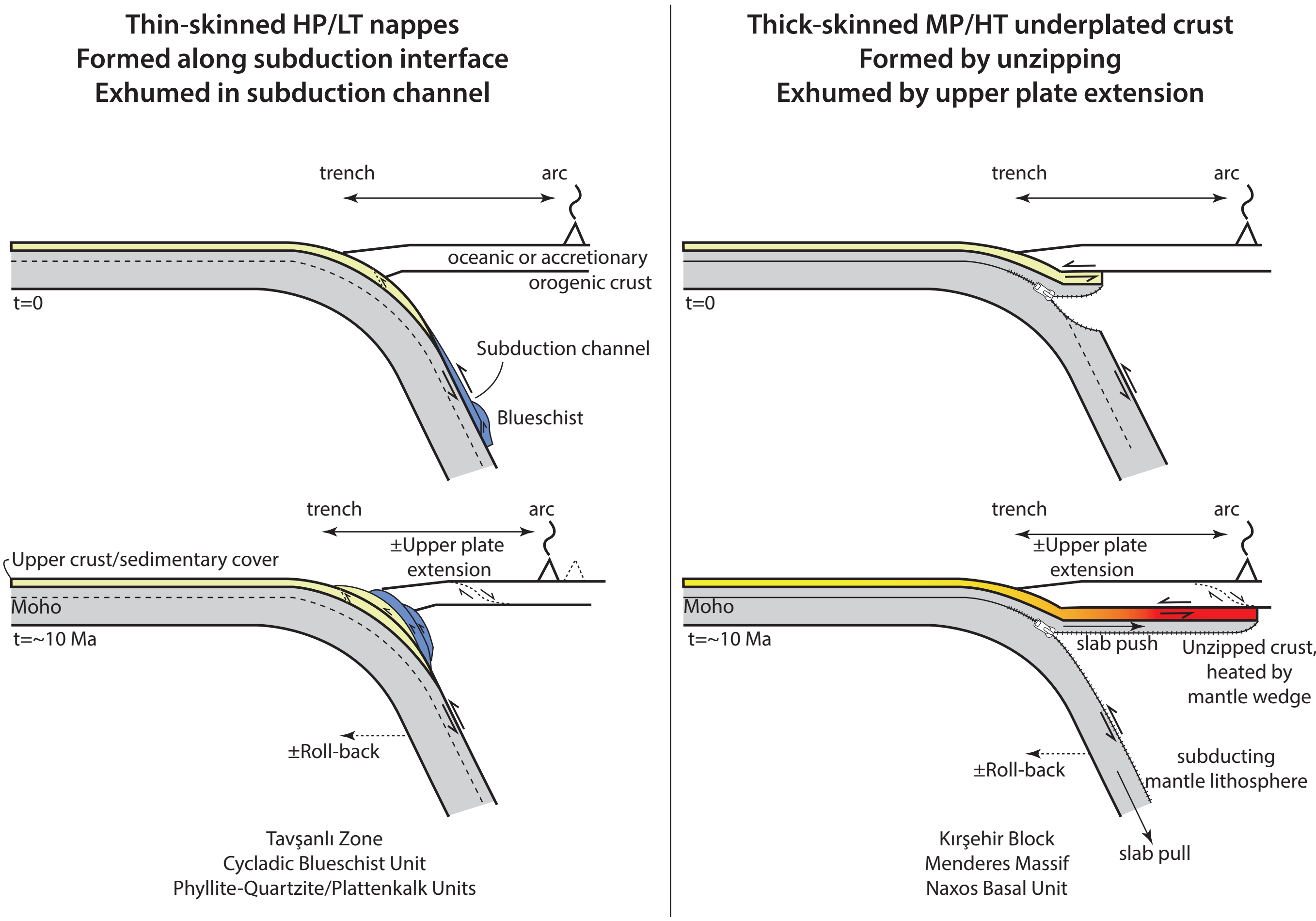

Thin-skinned HP/LT nappes
Formed along subduction interface
Exhumed in subduction channel
Thick-skinned MP/HT underplated crust
Formed by unzipping
Exhumed by upper plate extension
trench
arc
oceanic or accretionary
orogenic crust
t=0
Subduction channel
Blueschist
trench
arc
t=0
trench
arc
±Upper plate
extension
Upper crust/sedimentary cover
Moho
t=~10 Ma
±Roll-back
Tavşanlı Zone
Cycladic Blueschist Unit
Phyllite-Quartzite/Plattenkalk Units
trench
arc
±Upper plate
extension
Moho
t=~10 Ma
slab push
Unzipped crust,
heated by
mantle wedge
subducting
mantle lithosphere
±Roll-back
slab pull
Kırşehir Block
Menderes Massif
Naxos Basal Unit

**Figure 4.**

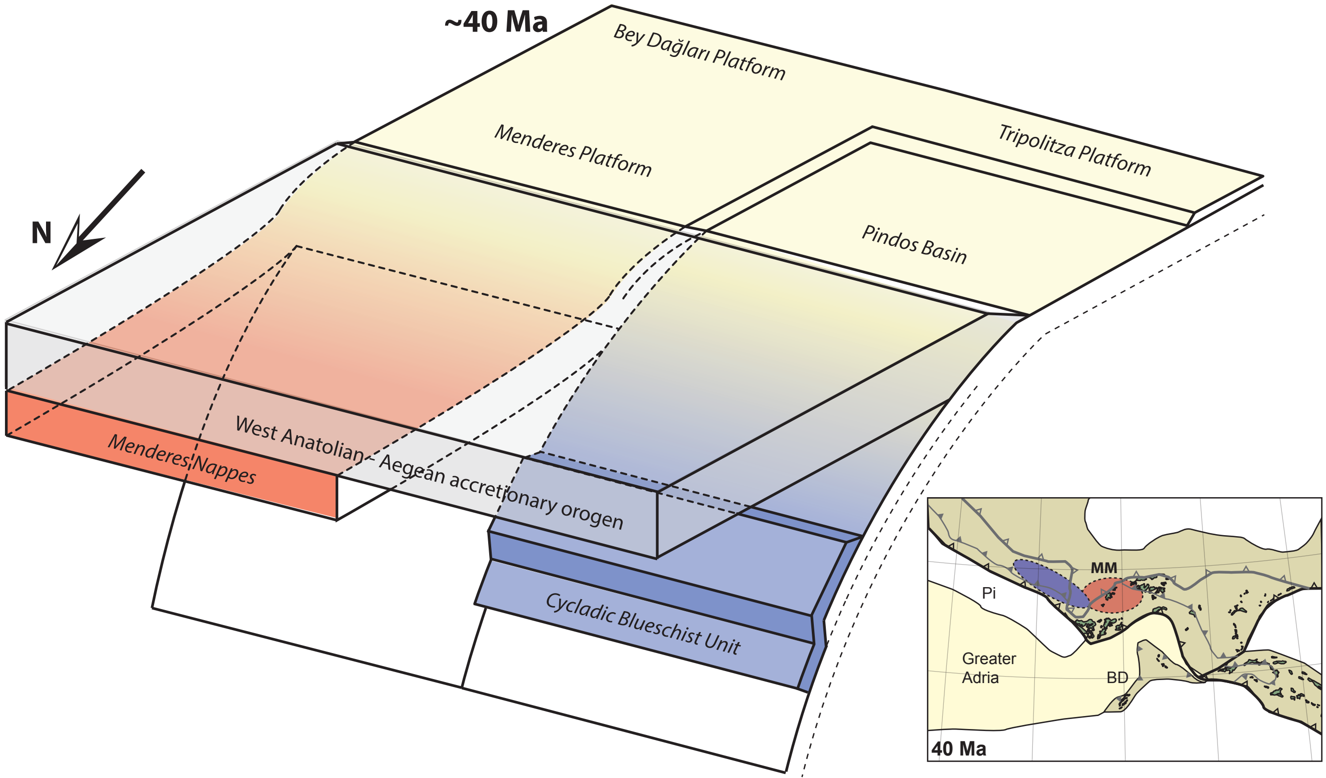
~40 Ma
Bey Dağları Platform
Menderes Platform
Tripolitza Platform
Pindos Basin
N
West Anatolian - Aegean accretionary orogen
Menderes Nappes
Cycladic Blueschist Unit
MM
Pi
Greater
Adria
BD
40 Ma

**Figure 5.**

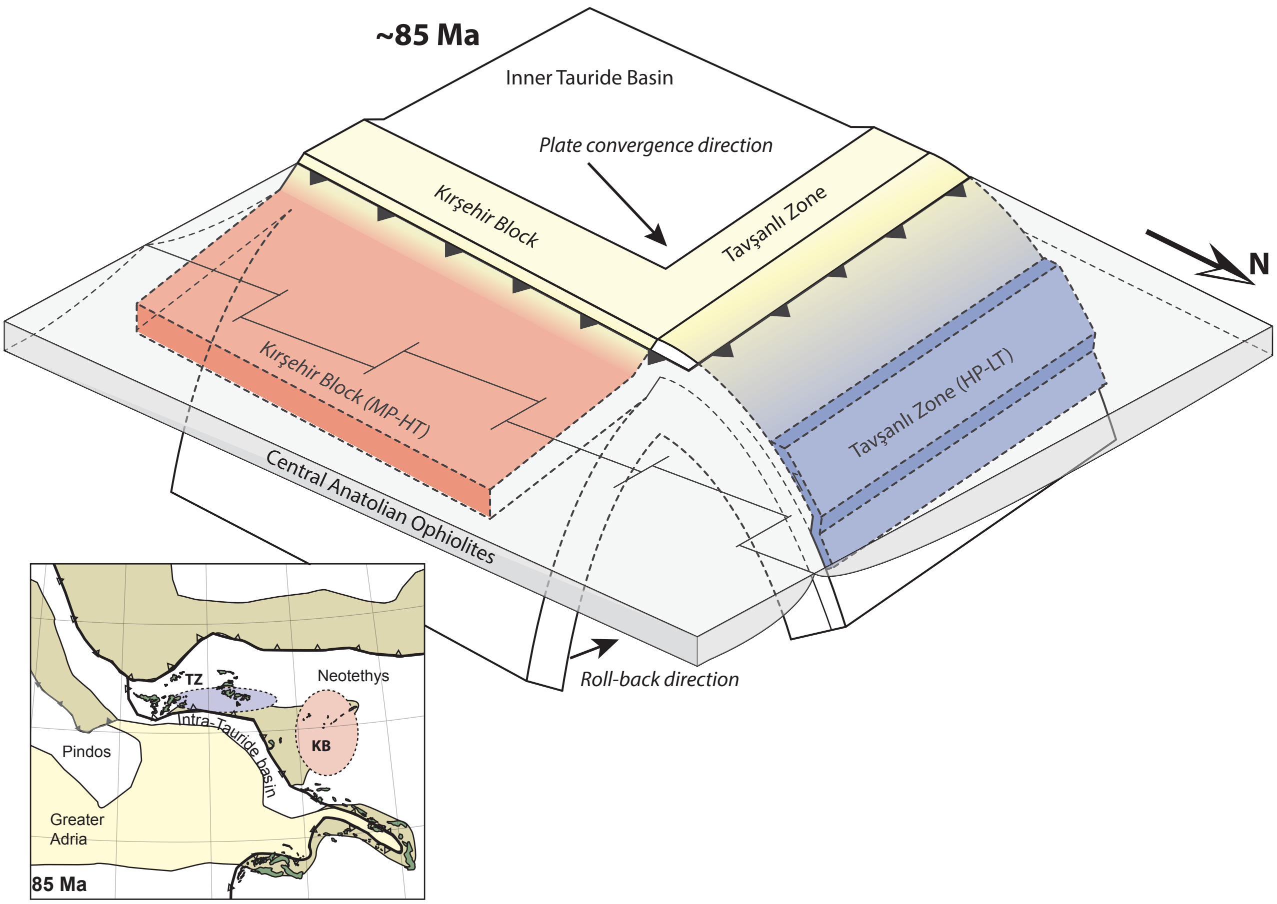
~85 Ma
Inner Tauride Basin
Plate convergence direction
Kırşehir Block
Tavşanlı Zone
N
Kırşehir Block (MP-HT)
Tavşanlı Zone (HP-LT)
Central Anatolian Ophiolites
Roll-back direction
TZ
Neotethys
KB
Intra-Tauride basin
Pindos
Greater
Adria
85 Ma

**Figure 6.**

**Simultaneous formation Phyllite-Quartzite HP-LT and Naxos Basal Unit MP-HT nappes**

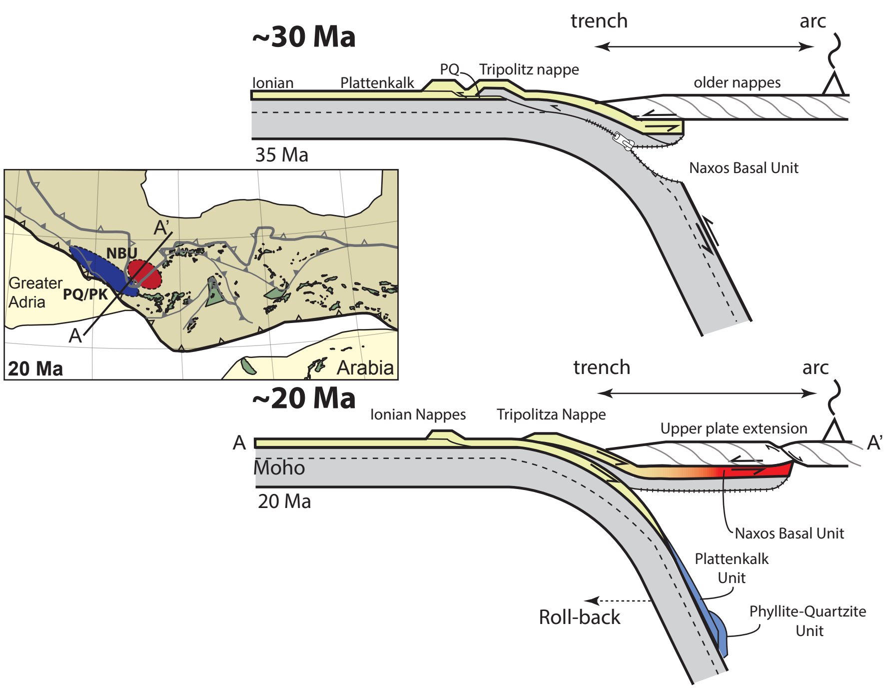

**Figure 7.**

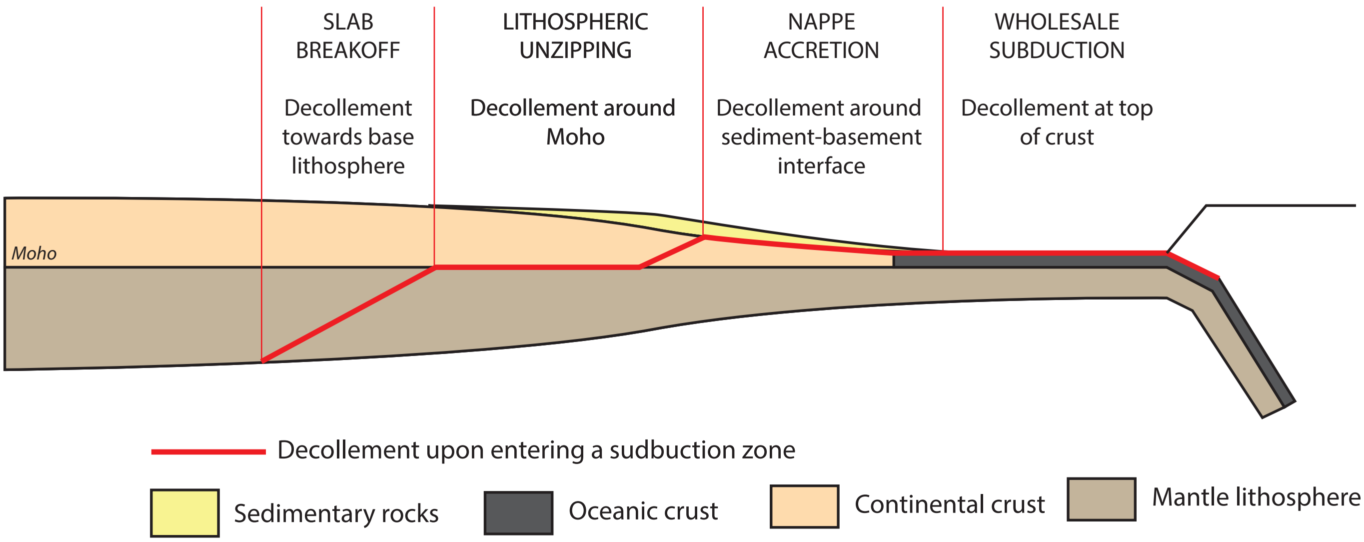
SLAB
BREAKOFF
Decollement
towards base
lithosphere
LITHOSPHERIC
UNZIPPING
Decollement around
Moho
NAPPE
ACCRETION
Decollement around
sediment-basement
interface
WHOLESALE
SUBDUCTION
Decollement at top
of crust
Moho
Decollement upon entering a sudbuction zone
Sedimentary rocks
Oceanic crust
Continental crust
Mantle lithosphere

**Figure 8.**

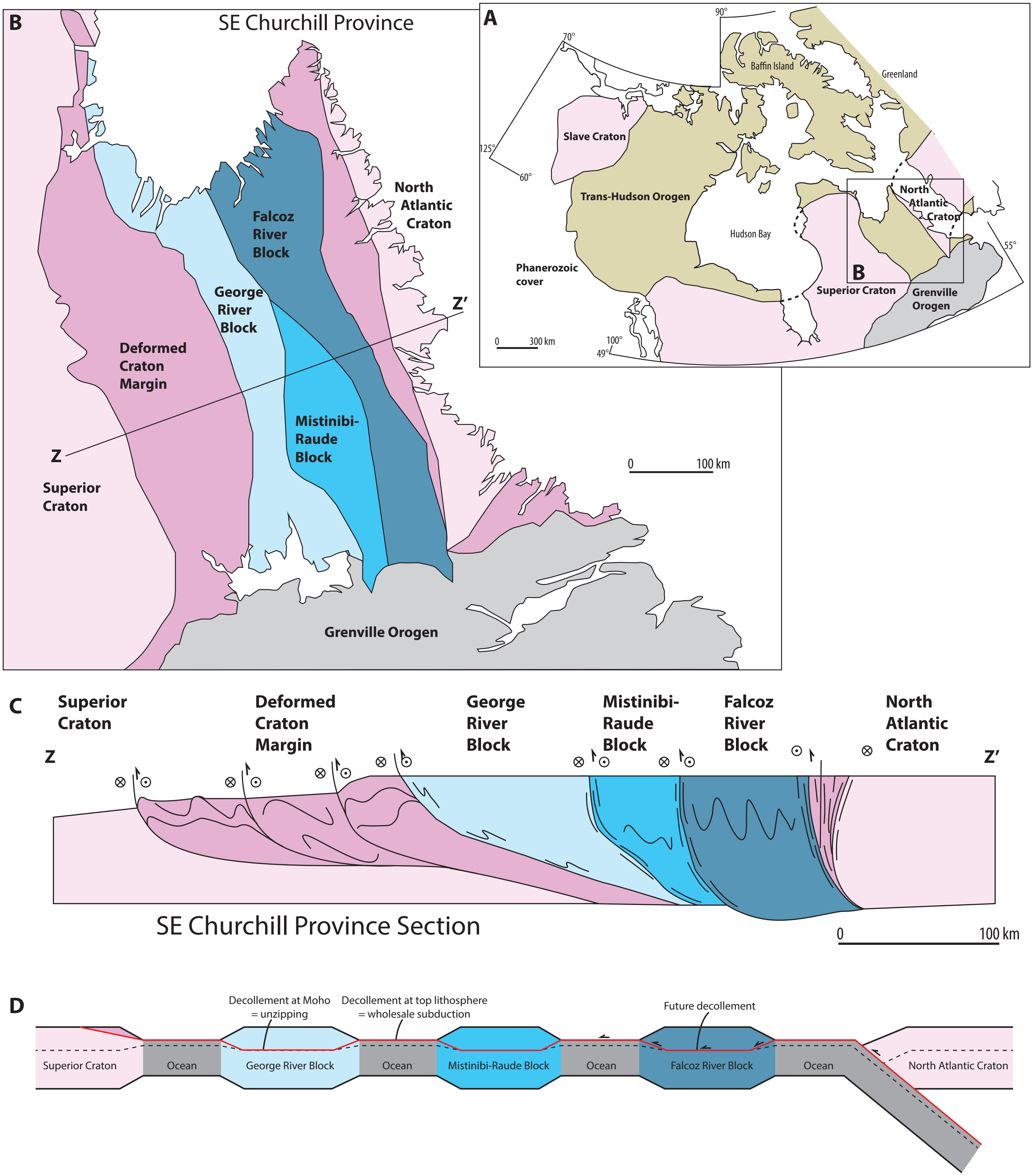

A
90°
70°
125°
60°
Baffin Island
Greenland
Slave Craton
Trans-Hudson Orogen
North Atlantic Craton
Hudson Bay
Phanerozoic cover
55°
B
Superior Craton
Grenville Orogen
0 300 km
100°
49°
B
SE Churchill Province
Falcoz River Block
North Atlantic Craton
George River Block
Z′
Deformed Craton Margin
Mistinibi-Raude Block
Z
Superior Craton
0 100 km
Grenville Orogen
C
Superior Craton
Deformed Craton Margin
George River Block
Mistinibi-Raude Block
Falcoz River Block
North Atlantic Craton
Z
Z′
SE Churchill Province Section
0 100 km
D
Decollement at Moho = unzipping
Decollement at top lithosphere = wholesale subduction
Future decollement
Superior Craton
Ocean
George River Block
Ocean
Mistinibi-Raude Block
Ocean
Falcoz River Block
Ocean
North Atlantic Craton